



Cite this: DOI: 10.1039/c8ta07125j

Blue energy harvesting on nanostructured carbon materials

Guohua Liu,^a Ting Chen,^b Jinliang Xu^{*a} and Kaiying Wang^{id}^{*c}

The generation of electric power from the relative movement of liquid and solid media is an attractive renewable energy strategy. From the interaction of water with nanostructured carbon substrates, low-power electricity has been observed on carbon nanotubes, carbon black film, graphene and their derivatives. Devices for harvesting electric power have diverse working principles in the literature, even though only electrons, water molecules and/or ions are involved in energy conversion. Therefore, a complete understanding of the energy conversion mechanism is critical for the future design of novel devices. In this report, we focus on the concept of harvesting energy from water–carbon interfaces and summarize the materials, structural design and electricity harvesting mechanism of devices. Three promising mechanisms of nanogenerators, namely, sliding droplets, flowing water and phase change processes, are discussed as responses to external stimuli. Moreover, their physical characteristics are analyzed in depth to understand the state of the art in device design. We envisage that a better understanding of carbon-enabled devices would inspire the design of highly efficient miniaturized power systems for the water–energy nexus.

Received 24th July 2018
Accepted 6th September 2018

DOI: 10.1039/c8ta07125j

rsc.li/materials-a

1. Introduction

Harvesting energy from the ambient environment, such as light,¹ heat,² wind,³ acoustic waves,⁴ vibrations,⁵ human movements,⁶ and water waves,⁷ is an interesting and attractive strategy for meeting the demand for energy.^{8–10} Natural water on the Earth brings about gigantic movements of energy (blue

energy), such as raindrops, river flow and ocean tides. Harvesting blue energy provides a viable source of renewable energy, as well as a potential basis for novel self-powered systems.^{11,12} This energy harvesting technology can be applied in a variety of circumstances wherever electricity is required without an external power source, including water desalination and purification, corrosion protection and wireless sensing, and can even feasibly be implanted in personal or medical devices.^{13–17} Conventionally, dams and waterwheels have been built to harvest energy from flowing water, by which mechanical energy derived from water is transformed into electricity.¹⁸ However, these facilities are usually heavy and complex, and specific sites with large differences in altitude are required for efficient operations. Low-frequency kinetic energy such as

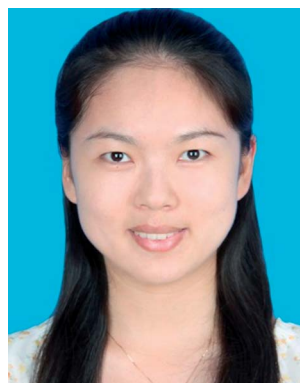
^aBeijing Key Laboratory of Multiphase Flow and Heat Transfer for Low Grade Energy Utilization, North China Electric Power University, Beijing 102206, China. E-mail: xjl@ncepu.edu.cn

^bSchool of Chemical and Environmental Engineering, Jiangnan University, Wuhan 430056, PR China

^cDepartment of Microsystems, University of South-Eastern Norway, Horten 3184, Norway. E-mail: Kaiying.Wang@usn.no



Guohua Liu received his PhD in Engineering of Thermophysics from the Chinese Academy of Sciences in 2010. He obtained his second PhD in Micro and Nano Systems Technology at the University of South-Eastern Norway (USN) in 2013. Currently, he is a full professor at North China Electric Power University. His research interests center on the development of nanostructured materials for energy applications.



Ting Chen received her PhD in Materials Physics and Chemistry from Sun Yat-sen University in 2014. Currently, she is working at Jiangnan University as a full faculty member. Her research interests are centered on the development of nanostructured materials for energy applications and the design and optimization of chemical engineering processes.

raindrops, river flow and ocean tides cannot be harnessed sufficiently. Therefore, novel designs of efficient and miniaturized energy harvesting systems are desirable for surmounting these limitations.¹⁹

With advances in nanotechnology, small devices have been developed for harvesting blue energy. Nanodevices generally harvest energy *via* the piezoelectric effect or triboelectric effect.^{12,20} When a piezoelectric device is subjected to compressive stress, the induced piezopotential drives a transient flow of electrons to produce electricity. Commonly used materials in devices include ZnO, GaN and PVDF (polyvinylidene fluoride). A triboelectric device converts mechanical energy into electricity *via* the combined effects of triboelectrification and electrostatic induction as a result of the contact and separation of two materials with opposite tribopolarity. PDMS (polydimethylsiloxane), PMMA (polymethyl methacrylate), and PTFE (polytetrafluoroethylene), as well as metals, are commonly used materials.²¹ Recently, carbon-based nanomaterials have sparked tremendous interest in harvesting blue energy. For example, moving droplets of ion-containing water over graphene induce a potential along the direction of flow.^{22,23} Ionic and nonionic liquids that flow inside or outside carbon nanotubes or over graphene also produce electricity.^{24–26} Transient potentials can also be generated by the evaporation of water or adsorption of moisture in carbon films.^{27–29}

Carbon nanomaterials have attracted more interest than other materials owing to their high electrical conductivity, low cost and versatile forms such as powders, tubes, fibers, composites, 2D thin films and 3D foams.^{30–32} More importantly, their high chemical stability in different solutions and ability to perform over a wide range of temperatures increase the desirability of these materials. Current methods of activation enable the production of porous carbons with large surface areas, which provide large electrode/electrolyte interfaces for charge storage. Their unique electrical properties with well-controlled pore sizes and structures facilitate the fast transport of ions and electrons.^{9,33} In addition, the incorporation of well-defined carbon materials into devices provides advantages such as simple assembly, flexibility and high structural stability.

However, carbon materials exhibit strong charge interactions with neighboring materials or their substrates.^{34–38} Many interesting effects such as the adsorption of anions in electrolyte solutions, the Seebeck coefficient between different types of doping sheets, the strain energy band effect and ion channels in networks dramatically influence the generation of electricity.^{21,39–47} This results in different operating principles in the energy conversion process, even though only electrons, water molecules and ions are involved. Although different mechanisms have been suggested to understand the origin of electricity, such as friction with moving liquids,⁴⁸ electron drag,⁴⁹ drifting of absorbed ions,^{50,51} fluctuating asymmetric potentials and streaming potentials,^{24,52} coulombic drag,⁵³ pseudocapacitive effects,²² waving potentials,⁵⁴ adsorption potentials^{29,55} and evaporation potentials,^{27,56,57} the overall mechanism of energy harvesting remains unclear and controversial.^{16,21,58}

In this work, we summarize experimental advances in, as well as the physical understanding of, the development of carbon-based nanogenerators for the water-energy nexus. Devices are classified in terms of their external stimuli, such as droplet-based generators, flow-induced generators and phase change generators (Fig. 1). These novel water-carbon systems are then discussed in terms of particular forms used for harvesting blue energy, such as sliding droplets, rain, waves, shaking, circling or flowing water, and phase change processes such as the adsorption of moisture and evaporation of water. This is different from traditional harvesting of blue energy, which focuses on a difference in salt concentration.^{11,59,60} In addition, the physical mechanisms are analyzed in depth to guide the future design of miniaturized power systems. Finally, the report concludes with a summary of achievements and a few perspectives on remaining challenges.

2. Electricity generation from water-carbon interfaces

2.1. Droplet-based power generators

2.1.1. Single sliding droplet. The introduction of functional substances on monolayer graphene has attracted intensive



Jinliang Xu is the Dean of the School of Mechanical and Power Engineering, North China Electric Power University, China. His research interests focus on micro/nano heat transfer, micro energy systems, and multiphase flow and heat transfer. He has published more than 100 papers in recognized academic journals. He has served as the chair or co-chair of international conferences in related areas several times.



Kaiying Wang received his PhD in condensed matter physics from the Institute of Physics, Chinese Academy of Sciences in 1995. He joined the University of South-Eastern Norway in 2007 as an associate professor and was then promoted to professor in 2010. His research interests focus on microfabrication and nanotechnology, functional thin films, magnetic and superconductive materials, the character-

ization of nanostructures and nanodevices for environment and energy applications.

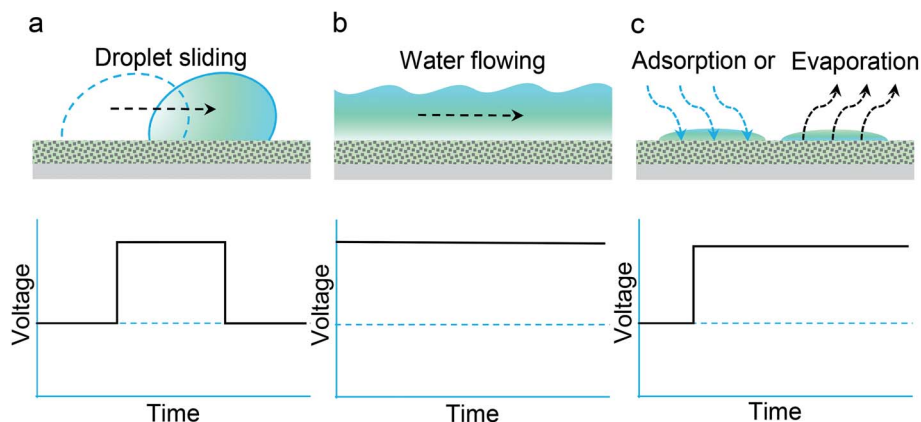


Fig. 1 Different forms of the motion of water along carbon materials and the corresponding results in terms of electricity generation. (a) Sliding droplets or rain. (b) Continuously flowing or waving water. (c) Moisture adsorption or water evaporation.

attention owing to their diverse physicochemical behavior.⁶¹ The interaction between graphene and electrolytes offers promising potential for the design of a range of electric power and energy devices. Notably, a voltage of a few millivolts was produced by moving an ionic droplet (NaCl solution) along monolayer graphene.²² The droplet was sandwiched between the graphene surface and an SiO₂/Si wafer (Fig. 2a) and was drawn along by the wafer. The induced voltage had the same magnitude when the droplet slid back and forth (Fig. 2b). The slight delay in the electric signal in response to the movement was due to contact angle hysteresis. Density functional theory calculations disclose that hydrated Na⁺ cations are adsorbed on the graphene surface because of its positive adsorption energy. With an increase in the amount of adsorbed Na⁺, a thin layer of accumulated electrons is distributed along the contact surface of graphene, and a pseudocapacitor is formed at the graphene/liquid interface. Traditionally, the term pseudocapacitor refers

to a specific type of electrochemical capacitor that stores electrical energy *via* faradaic redox reactions.⁶² Here, the capacitor is a configuration with similar behavior, which is driven forward by the movement of the droplet, which results in the migration of electrons in graphene. Considering the dynamic front and rear boundaries of the droplet as capacitors in charging and discharging modes (Fig. 2c), ions are adsorbed at the front and desorbed at the rear, which decreases or increases the electron density and leads to a potential difference. The induced potential depends on the number and velocity of droplets as well as the ionic species and their concentration and decreases sharply with an increase in the number of graphene layers.

In contrast to monolayer graphene, van der Waals heterostructures consist of stacks of multiple two-dimensional layers. The in-plane stability of each layer is maintained by strong covalent bonds, whereas the stack is held together by weak van der Waals forces. The van der Waals interactions induce

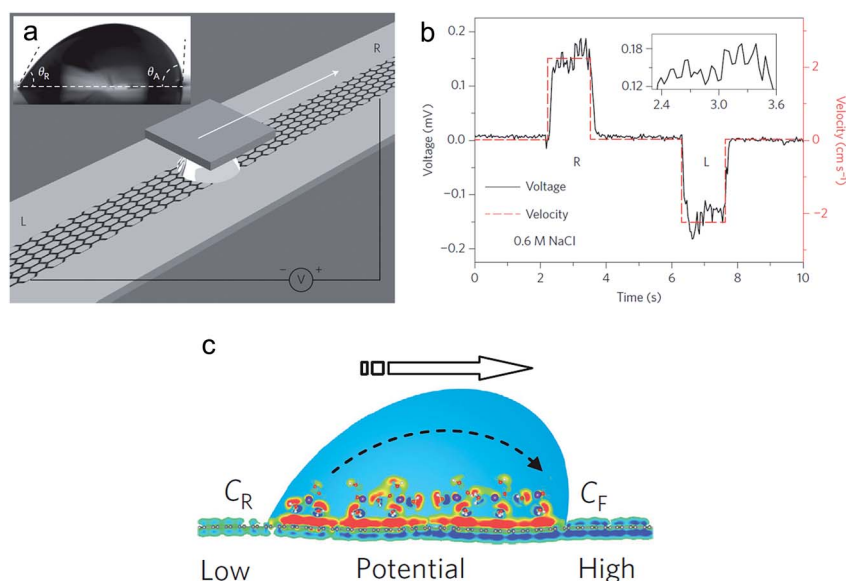


Fig. 2 (a) Sliding droplet device. (b) Voltage signals produced by drawing a droplet along from left to right and backward. (c) Potential difference induced by a moving droplet. Reproduced with permission.²² Copyright 2014 Nature Publishing Group.

different mobilities of carriers in and out of the lattice plane, and thus the asymmetric carrier transport leads to interesting effects.⁶³ An electrical response was observed by moving a droplet of an aqueous solution of graphene oxide (GO) on monolayer graphene.^{51,64} Fig. 3a shows the voltage response to the movement of a droplet of deionized water and a 0.5 mg mL⁻¹ aqueous solution of GO, respectively. No electrical response could be detected when the water droplet was moving along the graphene layer, whereas the voltage remained around 0.11 mV in the case of the aqueous solution of GO. The fluctuations in the voltage signals were caused by fluctuations in movement. When GO droplets move along a graphene surface, holes in the graphene layer are dragged along by frictional coupling. This coupling is caused by Coulomb scattering between moving negatively charged centers in GO and holes in p-type doped graphene, which leads to the transfer of momentum between the layers. To balance the motion of the holes, a corresponding longitudinal voltage is induced in the underlying graphene layer, which gives rise to a potential difference along the direction of movement (Fig. 3b).

Piezoelectric techniques are efficient methods for converting mechanical energy into electricity when a device is subjected to an external force. Sliding a small droplet of DI water over a graphene-coated piezoelectric substrate gives rise to an obvious voltage signal.³⁶ The voltage is proportional to the polarity of the water, resistance of the graphene, and piezoelectric constant of the substrate to a certain extent, but decreases sharply with an increase in the number of graphene layers. Electrokinetics cannot explain this phenomenon, because there is no electrical response to the flow of DI water.²² According to piezotronics, when water beads are dropped onto a graphene surface, electrical charges are induced on the film surface as a result of the dropping pressure. Charge carriers with opposite charges accumulate at the water-graphene interface (Fig. 4a). When a droplet is sliding, piezoelectric charges are generated at the front end of the water droplet, which draw electrons along in the graphene and result in a decrease in electron density ahead of the water droplet and an increase in electron density behind the droplet (Fig. 4b). This leads to a higher electron density in the area of graphene behind the droplet than that ahead of the droplet,

which results in a potential difference (Fig. 4c). The dynamic carrier attraction and release processes can be described in terms of two capacitors that form at the piezoelectric material-graphene interface and water-graphene interface, respectively (Fig. 4d). Therefore, the potential arises from a continuous charging-discharging process in graphene that is a result of the relative accumulation of ions at the rear of the water droplet (retarded screening effect) due to the generated piezoelectric charges.

Triboelectric charging is a form of contact electrification in which certain materials become electrically charged after they come into frictional contact with another material. The contact-induced charges can generate a drop in potential between the materials.²⁰ For instance, a negative triboelectric potential is created on the polytetrafluoroethylene surface when a graphene layer is transferred to a polytetrafluoroethylene substrate. If a droplet of an NaCl solution slides on a graphene/polytetrafluoroethylene surface, accumulation of positive and negative charges would occur on the bottom and top surfaces of graphene, respectively, as a result of the triboelectric potential. The negative charges that accumulated on the top surface of graphene are then driven forward by the moving droplet. After the water droplet achieves a constant speed, cations inside the water droplet accumulate at the front of the droplet. Owing to this accumulation of cations, the uniform balance of surface charges in graphene is disrupted, which induces a relative difference in potential between the two ends of the droplet. This potential difference further triggers the migration of electrons from the front and rear of the droplet. This change in triboelectrification-induced pseudocapacitance between the water droplet and monolayer graphene can be optimized to produce a power output of 1.9 μ W.⁶⁵

2.1.2. Intermittent raining droplets. Natural raindrops contain positively and negatively charged ions. When raindrops fall onto a graphene surface, they spread quickly to form p-electron/cation electrical double-layer (EDL) pseudocapacitors at the graphene-raindrop interface (Fig. 5a). Delocalized electrons are dragged forward and backward by the spreading and shrinkage of raindrops, which charges and discharges the pseudocapacitors. These charging-discharging processes would lead to the generation of current and voltage signals by

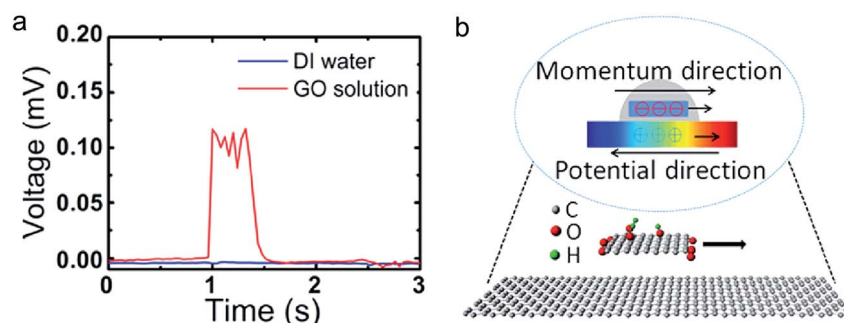


Fig. 3 (a) Voltage responses to the movement of a droplet of DI water or an aqueous solution of GO. (b) Moving van der Waals heterostructure and momentum transfer process induced by the Coulomb interaction between charged GO nanosheets and carriers in 2D graphene. Reproduced with permission.⁶⁴ Copyright 2015 American Institute of Physics.

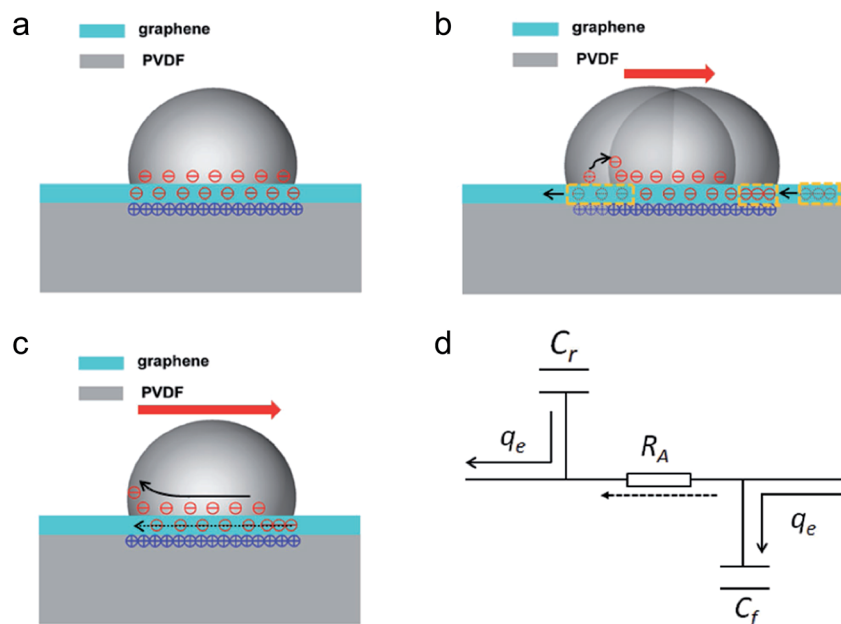


Fig. 4 (a) Charge distribution in the static state. (b) Dynamic charging–discharging process. (c) Overall charge transfer process; carriers in graphene are dragged along and move from the front to the rear. (d) Equivalent circuit. Reproduced with permission.³⁶ Copyright 2017 Wiley-VCH.

intermittent raindrops. Carbon-based electrodes combined with solar cells have been designed for harvesting energy from sunlight and raindrops or steam.^{66–69} When a device was illuminated with simulated sunlight, the cell yielded a front power conversion efficiency of 6.53% and a rear efficiency of 4.26%. On rainy days, the energy harvesting panel is turned over with the reduced graphene oxide (rGO) film upward, which creates an electrical output as a result of the persistent dropping of raindrops. Preliminary results show that the signals are dependent on the lateral distance between the dropping position and rGO and the time interval between adjacent droplets, as well as the Na^+ concentration, and yield maximum values of *ca.* 0.50 μA , *ca.* 120 μV , and *ca.* 50 pW for each raindrop. However, this strategy is not a robust technique owing to the fragile and non-cohesive nature of the indium tin oxide (ITO)–polyethylene terephthalate substrate.

To integrate the device into a rigid substrate for practical applications, an all-weather cell was built on commercial fluorine-doped tin oxide glass, and subsequently a graphene film was deposited by electrophoretic deposition.⁷⁰ The resulting cell yielded a maximum photoelectric conversion efficiency of 9.14% under simulated sunlight.⁷¹ Simulation results indicate that the signals are strongly dependent on the injection velocity and cation concentration, and the maximum current, voltage, and power output were 4.9 μA , 62.0 μV , and 303.8 pW, respectively, on a rainy day. A remaining problem with this approach is the challenge of forming thin-film graphene for large-scale applications. The integration of graphene into insulating polymer matrices is a promising technique. A conducting composite coating of graphene/carbon black (G–CB) with PTFE has been fabricated to increase the film-forming ability, in which carbon black acts as a binder for compatibility

between graphene and PTFE and graphene forms percolation pathways for electron migration.²³ The bright regions in Fig. 5b indicate that the incorporated sericite powder formed interconnected networks within the composite. Electrical percolation that arises from the interconnection of the G–CB regions affects voltage outputs (Fig. 5c). When a raindrop spreads to the periphery, the cations in the raindrop drag absorbed electrons along, which migrate along percolation pathways and charge the pseudocapacitor. Subsequently, the electrons are released to graphene during the shrinkage process, which discharges the pseudocapacitor.

Simultaneously harvesting energy from sunlight and the flow of raindrops in one 2D material plane is useful for practical applications, because with this technology the panel does not need to be turned over. A graphene hybrid nanogenerator has been designed for this purpose.⁷² The generator is based on a graphene/silicon van der Waals Schottky diode. Two different metal electrodes are introduced to generate an asymmetric internal potential profile in the graphene channel, which enables the harvesting of energy from sunlight in the graphene plane with an output power of 49.3 mW. When a raindrop flows over the graphene surface under illumination, an additional voltage is produced. This flow-induced voltage arises from additional charge transfer in the graphene channel induced by continuous doping and dedoping of graphene owing to a reversible wetting and dewetting effect of water during the water sliding process. Fig. 6a shows the charge distribution in the diode under illumination. When DI water is in contact with graphene, the dipole moments of water molecules act as a local electric field and lead to the transfer of electrons from the graphene to water droplets. As a result, the graphene undergoes p-type doping. The Fermi level of the graphene

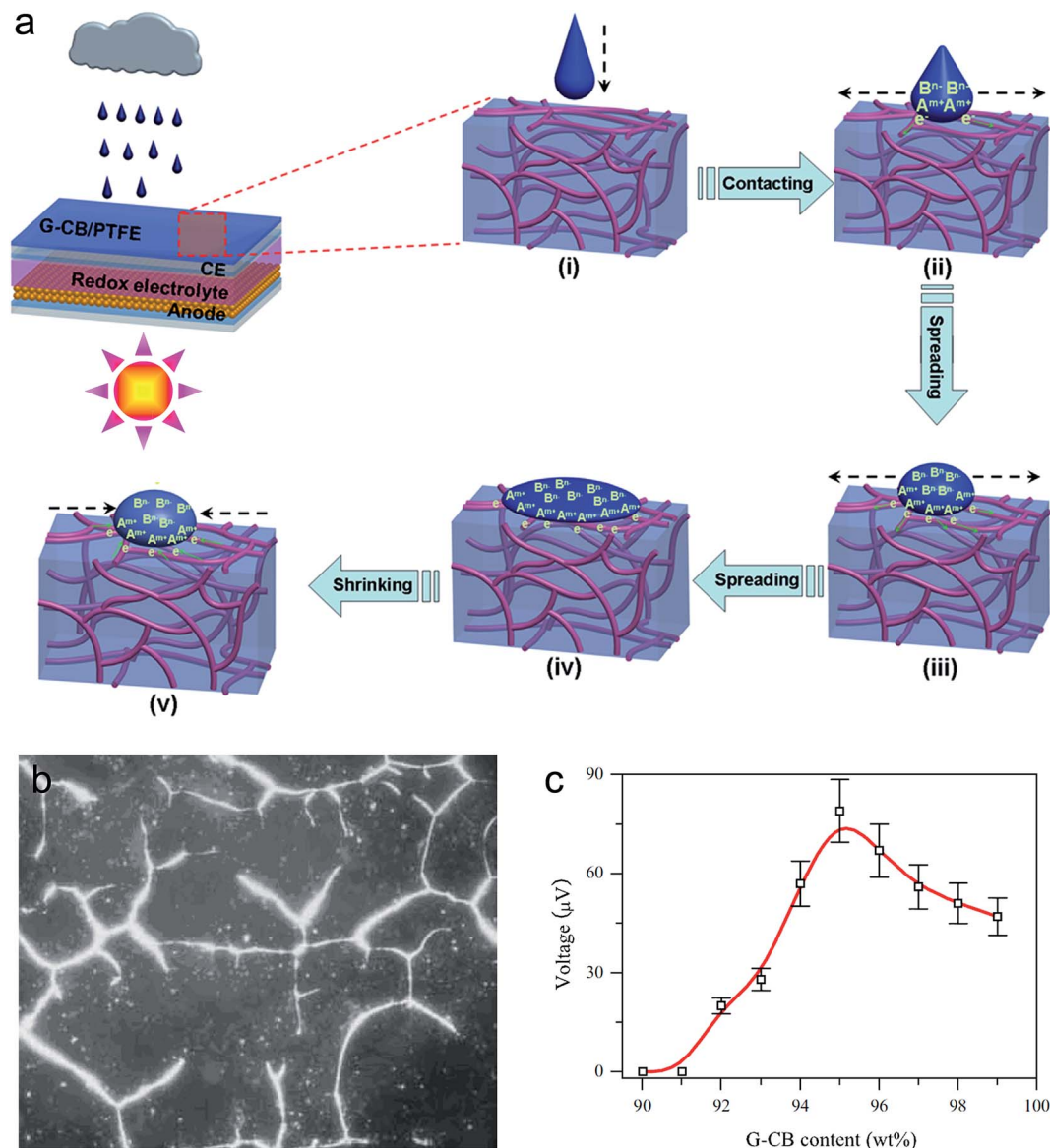


Fig. 5 (a) Pathways of charge adsorption and transport during the spreading/shrinkage processes of a raindrop on a conducting composite. (b) Polarizing microscopy image of polyacrylate/sericite composite. (c) Voltage signals induced by dropping raindrops on G-CB/PTFE electrodes. Reproduced with permission.²³ Copyright 2016 Elsevier.

shifts downward, the barrier in the diode becomes higher, the width of the depletion region in Si increases and more holes are pulled toward the graphene layer (Fig. 6b). When a droplet slides, the graphene channel at the front of the droplet is wetted and undergoes p-type doping by the water, and that at the rear of the droplet is dewetted and dedoped. Therefore, more holes are attracted to the front or repelled from the rear of the droplet (Fig. 6c). This dynamic process drives the excess holes in graphene to move from the rear to the front of the droplet, which leads to a potential difference (Fig. 6d). This example presents a physical picture of the dynamic adjustment of charge transfer characteristics by the flow of raindrops under solar illumination, which opens new prospects for practical applications.

2.2. Flow-induced power generators

2.2.1. Water waves and shaking water. Dynamic waves contain continuous kinetic energy. Capturing wave energy is an important method of powering smart devices in remote oceanic areas.¹⁴ Using nanomaterials to harvest wave energy is interesting in terms of cost and efficiency. It was reported that once a graphene sheet is immersed into an ionic solution and the liquid-gas boundary moves along the graphene sheet, a distinct voltage is induced without a pressure gradient. The experimental setup is shown in Fig. 7a.⁵⁴ In this approach, an electrode connected to the graphene sheet was carefully protected by silicone to avoid exposure to the solution. A waving potential was created by waving the water surface along the graphene sheet.^{54,73,74} This waving potential was proportional to the

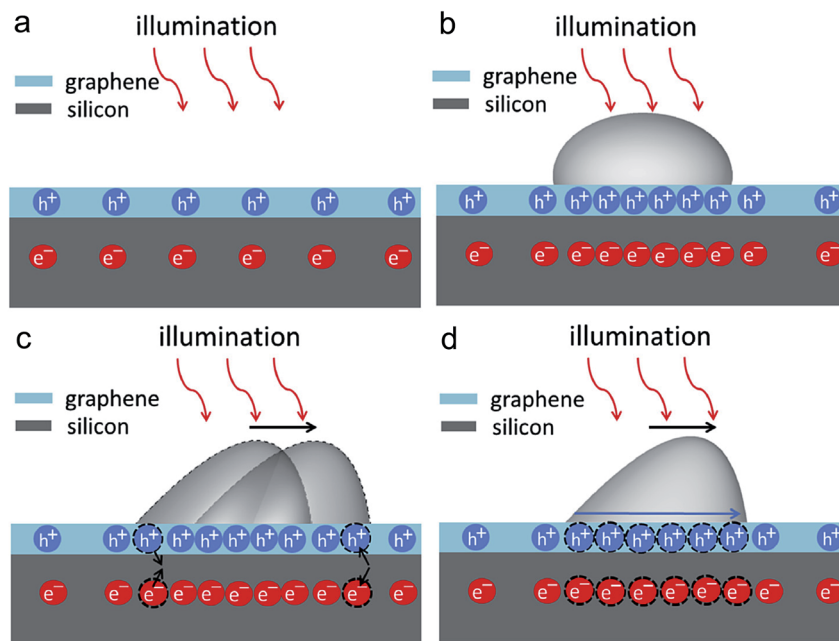


Fig. 6 (a) Charge distribution in the graphene/Si Schottky diode when under illumination. (b) Charge distribution in the water droplet/graphene/Si Schottky diode in the static state. (c) Dynamic charge transfer process in the diode when a water droplet is flowing along the graphene surface. (d) Overall charge transfer process in the graphene channel. Reproduced with permission.⁷² Copyright 2016 Elsevier.

insertion velocity and the number of graphene layers. On dipping into an NaCl solution, the induced voltage in a monolayer graphene sheet was one order of magnitude higher than that in a bi- or trilayer graphene sheet. A peak voltage of 3.3 mV was achieved by insertion or removal at a velocity of 3.1 cm s^{-1} (Fig. 7b). The voltage could be proportionally increased to more than 12 mV at a velocity of 40 cm s^{-1} (Fig. 7c). An open-circuit voltage of 0.1 V and a short-circuit current of $11 \mu\text{A}$ could also be obtained by parallel and series connections of devices. *Ab initio* molecular dynamics simulations indicate that the EDL of delocalized p-electrons adsorbed on the Na^+ layer and diffused on the Cl^- layer at the graphene/solution interface is created by a hole doping process (Fig. 7d). In the immersion process, the moving boundary of the EDL removes more electrons from graphene than at equilibrium, which results in a local concentration of holes and an electrical potential (Fig. 7e, left). Once the graphene sheet is completely immersed, the voltage drops to a resting value because no gas-liquid boundary exists. Similarly, removing the sheet drives the EDL boundary to move downwards and reverses the hole current (Fig. 7e, right).

Shaking is a horizontal fluctuation, which is different from the vertical movements of dipping or removal. Based on a van der Waals heterostructure, a graphene-based nanogenerator with asymmetric electrodes was built to harvest energy from the mechanical motion of shaking water (Fig. 8a).⁶⁴ A graphene monolayer was transferred onto a SiO_2/Si substrate with Au and Ag electrodes. The electrodes and copper wires were sealed with PDMS. The whole device was immersed in an aqueous solution of GO. A diagram of the electrical energy levels of this structure indicates a work function-based tuning mechanism (Fig. 8b), as the work functions of Au, graphene and Ag are 5.0,

4.6 and 4.26 eV, respectively. The discrepancy between the work functions results in a built-in potential difference that determines the direction of carrier transfer. When the bottle is shaken to excite fluctuations in water, the device produces electricity from a unidirectional flow of 2D GO nanosheets, which leads to a voltage output of $\sim 10 \text{ mV}$ and a current output of $\sim 0.5 \mu\text{A}$ (Fig. 8c and d). As there is an abundant amount of wave energy and shaking energy in the natural environment, this device is promising for practical applications.

The circling of water is a kind of omnidirectional movement. By a circling motion of the carbon material within a static solution, a generator based on multiwalled carbon nanotube (MWCNT) yarn has been observed to convert tensile energy in the yarn into electricity^{75,76} when an elastic coiled structure was obtained by creating an extreme twist in the CNT yarn. An output voltage was induced by a decrease in the capacitance of the coiled CNT yarn under an applied strain in an aqueous electrolyte (Fig. 9a). A reversible variation in the capacitance was caused by a change in the density of the yarn as a result of untwisting and twisting in the stretching and release processes. When a homochiral coiled yarn was stretched, the coils of the yarn would be partially converted into twists, which increased the density of the yarn. If stretched to a strain of 30%, the capacitance of the harvester decreased by 30.7% and its open-circuit voltage increased by 140 mV (Fig. 9b). The voltage decreased when a heterochiral yarn was stretched. This behavior of the twistrion was due to the large diameters of the MWNTs, bundling effects and the absence of pseudocapacitive redox-active groups. The bundled MWNTs partially collapsed to gain inter-nanotube van der Waals energy, which provided large pores to accommodate electrolyte ions (Fig. 9c and d).

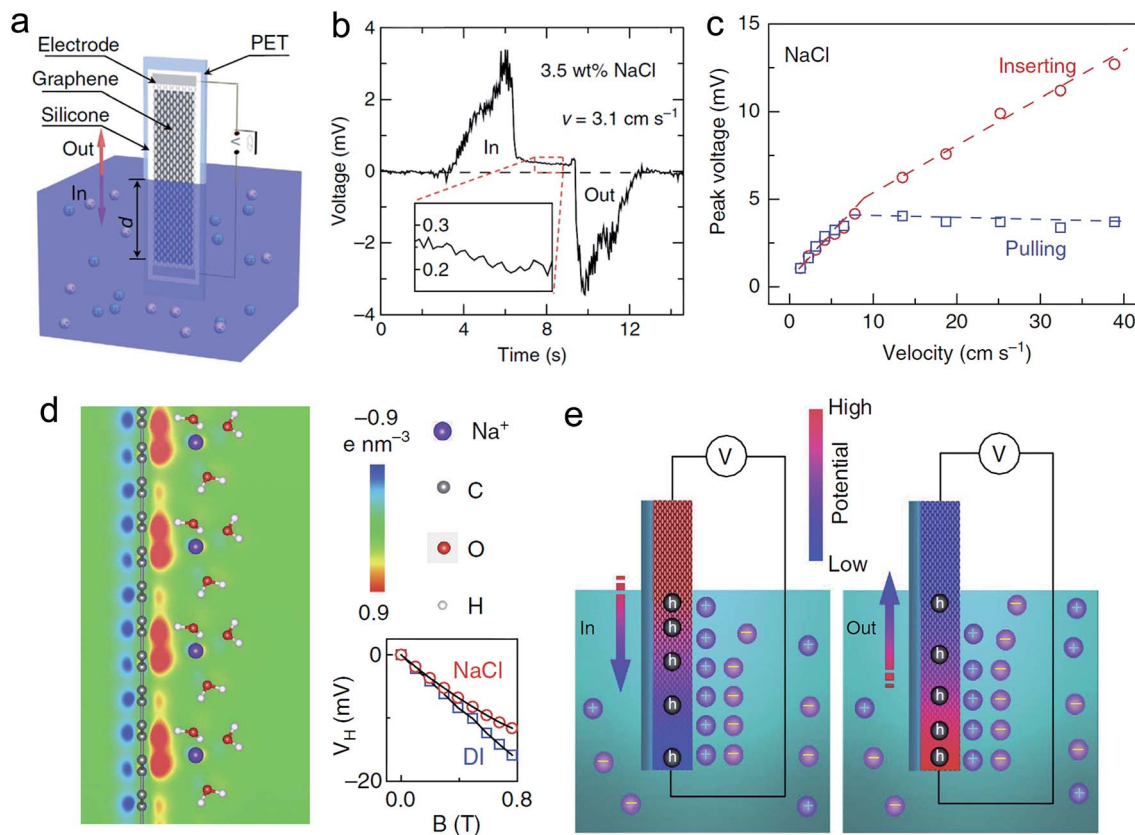


Fig. 7 Generation of waving potential. (a) Experimental setup comprising moving a graphene sample on a polyethylene terephthalate substrate vertically across the surface of water. (b) Voltage signals produced by inserting and removing the electrode. (c) Magnitudes of positive- and negative-peak voltages as functions of the movement velocity. (d) Charge distribution in graphene upon the adsorption of Na^+ ions. (e) EDL and its boundaries of ion adsorption (left) and desorption (right) on the surface of graphene during the insertion and removal processes. Reproduced with permission.⁵⁴ Copyright 2014 Nature Publishing Group.

2.2.2. Flowing water. The generation of flow-induced electricity by individual CNTs was first predicted theoretically in 2001.⁴⁸ Two mechanisms, namely, phonon drag and fluctuating coulombic fields, were examined for the flowing potential. Phonon drag comprises the transfer of momentum from molecules of a flowing liquid to acoustic phonons in the nanotubes, which drags free charge carriers along. The second mechanism comprises the direct scattering of free carriers by the fluctuating coulombic fields of molecules and ions in the flowing liquid. However, non-equilibrium phonon drag was identified as the dominant mechanism. Energy harvesting was achieved by flowing a liquid outside bundles of single-walled carbon nanotubes.^{24,77,78} An output voltage of 2.67 mV was generated in pure water at a flow velocity of 1.8 mm s⁻¹ and then increased fourfold with the addition of a 1.2 M HCl solution. The voltage displayed a strong dependence on the polarity of the liquid and the ion concentration and exhibited a logarithmic response to the flow velocity. Direct forcing of the free charge carriers in the nanotubes by the fluctuating coulombic field might be responsible for this nonlinear response.^{50,77} However, the fluctuating imbalance was perpendicular to the direction of flow, which was not consistent with the output voltage measured along the direction of flow.

A mechanism of streaming potential in porous materials is therefore proposed to explain the flow-induced potential. It is assumed that the treatment of CNTs by acid purification results in a negatively charged surface. Hence, the flowing liquid carried counterions near the liquid–solid interface, which was consistent with the sign of the experimental voltage.⁷⁹ Despite the ions, the electron drag effect and/or weak coupling between CNTs and water dipoles play a key role in producing electricity. Because ions and polar molecules in solution reinforce electron drag,⁸⁰ the dramatic increase in the voltage generated by the carbonized SWCNTs could be explained by electron drag on the surface due to ions or polar molecules in the solution.⁴⁹ Charge redistribution due to interactions between charge carriers and chains of water dipoles in the CNTs was considered as a possible mechanism of the flow-induced voltage in water-filled CNTs, and a voltage difference of 17.2 mV between the two ends of the tubes was predicted.²⁵ This calculation is in agreement with the experimental results, as an induced voltage of 8 mV was measured in water-filled single-walled CNTs.⁸¹ For gas flow, the underlying mechanism was assumed to be different from that in the case of liquid flow. The pressure difference along the streamlines gives rise to a temperature gradient across a sample, which in turn produces the measured

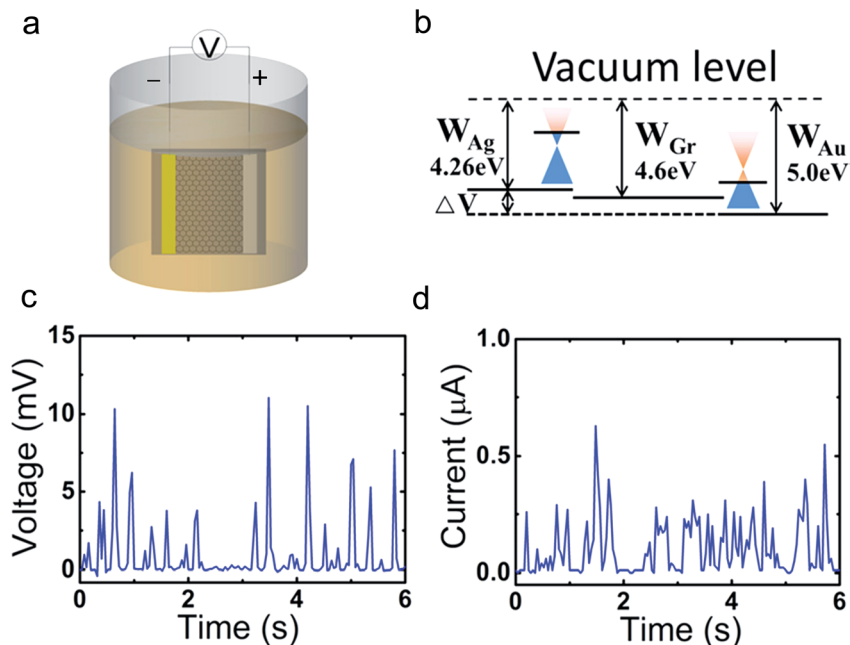


Fig. 8 Generation of shaking power. (a) Asymmetric electrode device. (b) Energy level diagram for contact between graphene and metals. The black solid lines indicate the intrinsic work functions of graphene and the metals. (c and d) Potential and current responses to slight shaking of the bottle. Reproduced with permission.⁶⁴ Copyright 2015 American Institute of Physics.

voltage as a result of the Seebeck effect.⁸² This effect is a phenomenon whereby a temperature difference between two dissimilar electrical conductors produces a voltage difference between the two substances.

The macroscopic assembly of CNTs provides a new route for improving their performance. A fluidic nanogenerator fiber (FFNG) with high flexibility has been fabricated from aligned multiwalled CNT sheets.⁸³ An EDL model is considered to be the

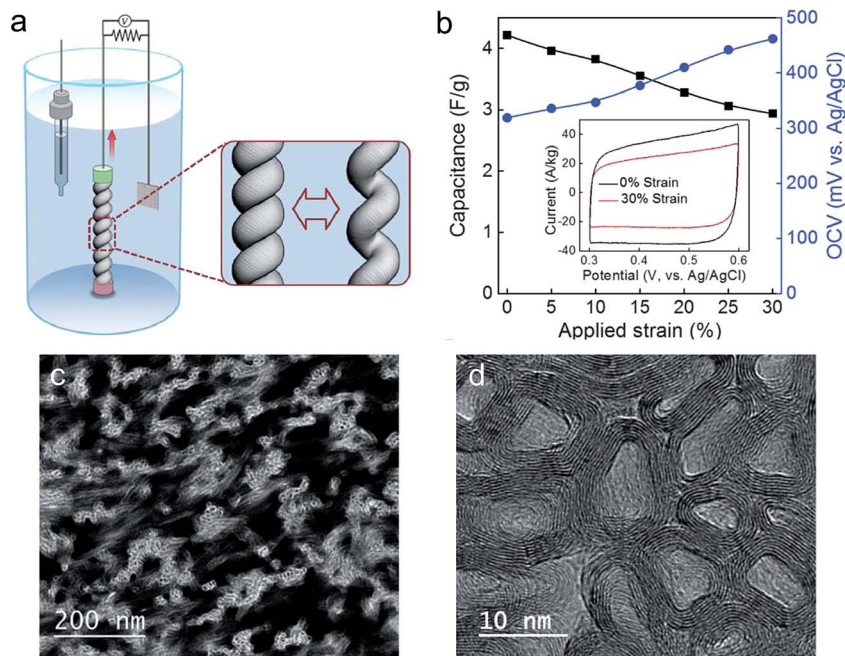


Fig. 9 (a) Coiled MWCNT yarn electrode, reference and counter electrodes in an electrochemical bath. The enlarged diagram shows the coiled yarn before and after stretching. (b) Capacitance and open-circuit voltage *versus* applied strain. The inset shows cyclic voltammograms for 0% and 30% strain. (c) TEM image of MWNT bundles and (d) image showing the collapse of MWNTs to increase the van der Waals energy. Reproduced with permission.⁷⁶ Copyright 2017 Science.

working principle of this device, in which an EDL forms at the interface between the CNTs and the fluid. A thin layer is formed by cations adsorbed onto the CNT surface because of the negative zeta potential. The net charge in this layer cannot be immediately counterbalanced by the anions at the front end of the fluid, which results in a charge imbalance along the fiber, which removes electrons from the CNTs to balance the excess charges. Unbalanced charges further accumulate in the front half of the device, which gives rise to a potential difference. The device exhibited both high efficiency and durability with a power conversion efficiency of 23.3%, which was well maintained after 1 000 000 cycles of deformation. The performance could be further improved by introducing ordered mesoporous carbon (OMC) into the interlayers among the MWCNT sheets. Owing to its large surface area, the OMC-FFNG provides a higher capacity for ion adsorption. Anions with larger radii are not easily attracted to the thin layer because of their lower electronegativity and larger volumes, which thus increases the output voltage. However, substitution with cations with different radii has little impact on the output voltage.

Graphene was recently suggested for flow-induced electricity applications. Flowing a 0.6 M HCl solution over few-layered graphene on an Si/SiO₂ substrate resulted in an induced voltage of 20 mV. Molecular dynamics simulations indicate that the generation of electricity is primarily caused by a net drift velocity of adsorbed Cl⁻ ions on the continuous graphene surface.²⁶ This mechanism requires the presence and transport of ions in the flow that drag charge carriers in graphene. The key supporting data for this interpretation are the saturation effect of the surface ion drift velocity, as well as the flow velocity.

However, Yin *et al.* found that no voltage was observed when the same solution flowed over graphene samples once the electrodes on graphene were isolated from the solution. The flow of water over a graphene-electrode system only produces voltages when both the graphene and the metal electrodes are exposed to the solution (Fig. 10a and b).⁸⁴ To isolate the electrodes from the solution, researchers modified the experimental setup so that the electrodes were aligned perpendicular to the flow of a non-ionic liquid. Measurements showed that a voltage was generated without electrode-solution interactions, which confirmed that the induced potential differences were due to an interaction with polar liquids and momentum transferred from the flowing liquid to the graphene layer.^{85,86} However, harvesting a voltage from an ionic liquid continuously flowing along graphene on the macroscale is still a challenge. A graphene grid with a network structure was therefore designed to produce a voltage of ~3.5 mV from the continuous flow of an ionic liquid over its rough surface (Fig. 10c).⁸⁷ This structure is effective for splitting a continuous fluid into droplets to generate a consistent voltage. When the liquid flows forward, charging and discharging of the pseudocapacitor occur around the bulges in the graphene grid, which confirms the electrochemical mechanism.

To crosscheck the dependence of the output current on the solvent polarity, the polarity was tuned by adjusting the ethanol/water volume ratio.⁸⁸ The induced current was reduced from 10 to 8 μ A by decreasing the polarity of an ethanol/water mixture from 10.2 to 8.73. This suggests that the induced current is closely related to the flow velocity and polarity of the mixture. Alternatively, pure water can be employed in 3D graphene frameworks for the generation of electricity (Fig. 10d), which

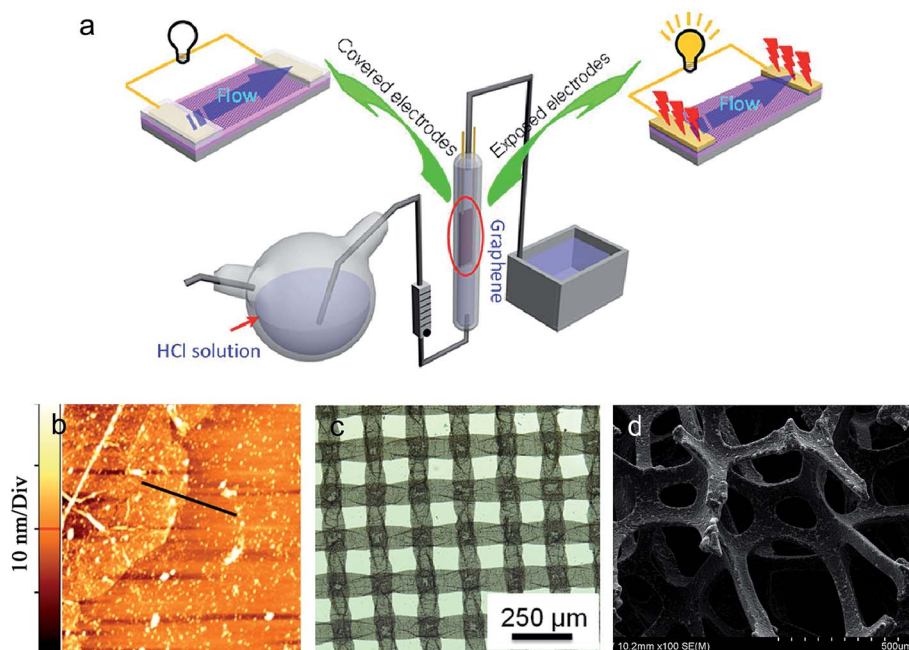


Fig. 10 (a) Generation of electricity by water flowing over graphene. Reproduced with permission.⁸⁴ Copyright 2012 American Chemical Society. (b) AFM line scan image along the edges of a few-layered graphene sheet indicates a sheet thickness in the range of ~2–3 nm. Reproduced with permission.²⁶ Copyright 2011 American Chemical Society. (c) Optical image of graphene grid and (d) SEM image of three-dimensional graphene on Ni foam. Reproduced with permission.⁸⁷ Copyright 2015 American Institute of Physics and Reproduced with permission.⁸⁸ Copyright 2011 American Chemical Society.

yielded a current of 10 μA at a zero bias at a flow velocity of 10 cm s^{-1} .⁸⁹ The increase in induced current displayed a nonlinear dependence on the flow velocity, but had no relationship with the flow direction and external bias voltage. The reason for the generation of current is attributed to the coupling interactions between chains of water dipoles and free charge carriers in the graphene foam. Free charge carriers are dragged along the direction of flow and form an induced current. The migration of free charges is accelerated at an increased velocity, which yields an increased current. However, why only a current instead of a voltage is produced is still unclear.

Lamellar structures with interconnected nanochannels within carbon membranes provide remarkable properties such as adequate mechanical strength and excellent ion selectivity. The interlayer nanocapillaries allow the unimpeded permeation of water, which results in an attractive force on cations or anions for the generation of electricity.^{90,91} A generator has been developed on the basis of electrokinetic ion transport through a layered graphene hydrogel membrane (Fig. 11a–c).⁹¹ In this case, nanocapillaries are formed between adjacent graphene

sheets, and a large-scale interconnected nanofluidic network is constructed. The transmembrane ionic conductance exhibits an exponential increase with an increase in the concentration of the electrolyte (Fig. 11d). This indicates surface-charge-governed ion transport through the graphene nanocapillaries. When an electrolyte flows through the graphene hydrogel membrane in a vertical direction driven by an external mechanical force, an electrokinetic phenomenon is observed in the form of the generation of a synchronous ion current across the membrane. Specifically, when a pressure difference of 5 kPa was applied, a continuous output current of 2.2 nA was obtained in a 0.1 M NaCl solution (Fig. 11e and f), and the maximum streaming conductance density approached 16.8 $\mu\text{A cm}^{-2}$ per bar. Both continuous and pulsed ion current signal can be obtained from this device, depending on the input mechanical wave. This strategy implies that this generator can be employed to harvest energy from footsteps and streams of bodily fluids.

It is difficult to generate electricity by continuously flowing a liquid over a carbon surface, as this normally requires modification of the surface in the form of nanopores or

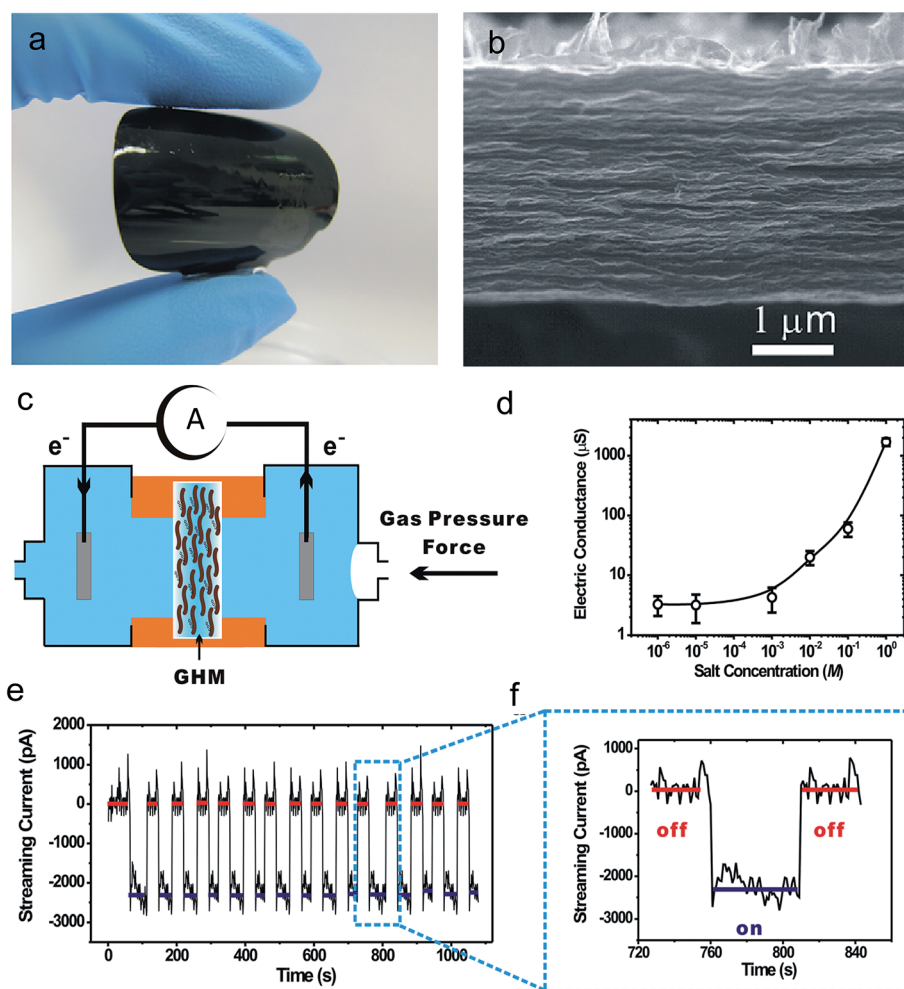


Fig. 11 Generation of electricity by a graphene hydrogel membrane. (a) A photograph of the membrane and (b) an SEM image of a cross-section show a layered structure. (c) Experimental setup. (d) The transmembrane ionic conductance is concentration-dependent and displays saturation. (e and f) When a continuous electrolyte flows across the membrane driven by a difference in gas pressure, a remarkable ion current is observed. A stable current output can be repeated by turning the electrolyte flow on and off. Reproduced with permission.⁹¹ Copyright 2013 Wiley-VCH.

intersecting network structures.^{87,89} To avoid the fabrication of complex structures, capillary flow of an electrolyte on a filter paper matrix has been proposed for power generation.⁹² Fig. 12a shows methods for the deposition of rGO and the experimental setup of a paper-pencil device. The porous paper channels drive flow *via* natural capillary action. The fibers and pores present in the paper form an intersecting network, which acts as a natural means of splitting a continuous flow into tiny droplets. Effectively, electrons are released at the anode and travel through the external circuit to reduce cations at the cathode and deliver an electrical output (Fig. 12b). The output voltage depends on the redox potentials of ionic species with various concentrations (Fig. 12c). A maximum current density of 325 mA cm^{-2} and a power density of 53 mW cm^{-2} were obtained using NaCl-DI water. The use of naturally available paper without the need for surface modification and the facile microfluidic approach used for depositing rGO over its surface are encouraging for the further development of energy devices.

2.3. Phase change power generators

2.3.1. Moisture adsorption. As well as liquid flow and sliding droplets, the motion of moisture also promotes the production of electricity in conductive polymers,⁹³ carbon films,²⁹ and GO frameworks.^{28,55,94} These carbon materials have large specific surface areas and are rich in oxygen-containing functional groups (*e.g.*, $-\text{OH}$ and $-\text{COOH}$) that can actively absorb abundant water molecules from air, which thus dissociate to give free mobile protons. An inner electrical potential is then formed in the materials when a difference in the proton concentration is produced by an inhomogeneous distribution of oxygen-containing functional groups.⁹⁵ It was found that GO stimuli-responsive systems are sensitive to moisture.^{96,97} The ionic and electronic conductivities of GO are dependent on the relative humidity (RH).^{96,98} This indicates that the interaction between oxygen-rich GO and water molecules is related to the material properties and functions of the final devices. In addition, a structure with a gradient in oxygen-containing groups was formed *via* a moisture-electric annealing process to

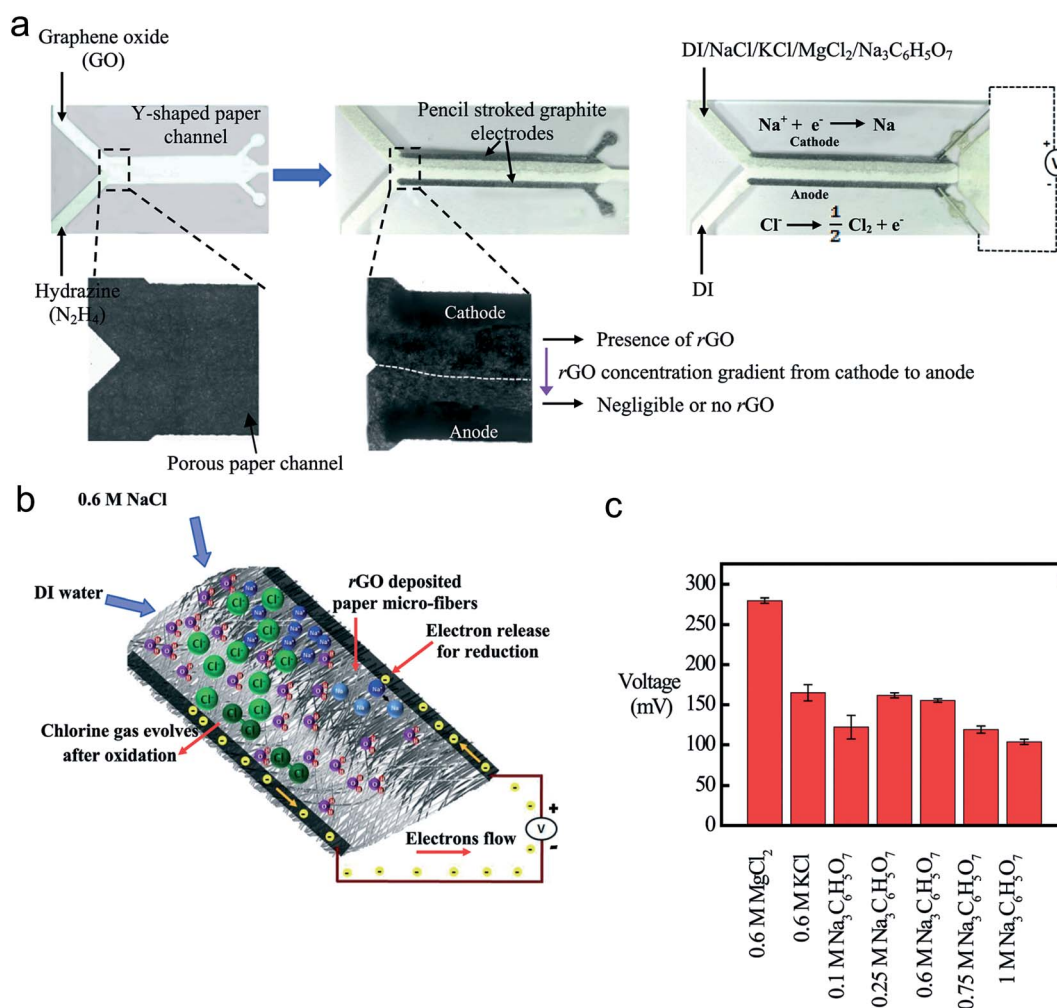


Fig. 12 (a) Paper-pencil device. (b) Electrochemical redox reactions of Na^+ and Cl^- ions occur at the respective graphite electrodes by the gain or loss of electrons. (c) The output voltage depends on the redox potentials of various ionic species. Reproduced with permission.⁹² Copyright 2016 Royal Society of Chemistry.

produce gradient graphene oxide (g-GO), in which a constant bias was applied between the two sides of a sample in an enclosed container with a relative humidity (RH), and thus the oxygen content of the sample gradually increased from the top to the bottom (Fig. 13a).^{28,55} The as-prepared Au/g-GO film/Au nanogenerator achieved an output voltage of 35 mV with a power density of 4.2 mW m^{-2} via the diffusion of moisture. More interestingly, a power-free respiratory monitor was developed by utilizing the flow of moisture in human breath as a renewable power source (Fig. 13b and c). As can be seen in Fig. 13d, calm breathing by a healthy man ($\Delta\text{RH} = 21\%$) provides an output voltage of 18 mV. After jogging, breathing is accelerated with an increase in ΔRH , and the output voltage increases to 20 or 30 mV. This respiratory energy collector converts energy provided by the body into electric power, which indicates the promising potential of the device. However, an obvious limitation on the output is caused by the limited adsorption of water on the compact layer structure of g-GO film.

A generator comprising a superhydrophilic three-dimensional assembly of GO Al/g-3D-GO/Al has therefore been fabricated to facilitate the diffusion of water molecules, as well as producing dissociated ions as free carriers. Moreover, its asymmetrical oxygen-containing groups enabled an ionic

gradient to accelerate the directed transport of ionic charge carriers. A high power density of *ca.* 1 mW cm^{-2} and an energy conversion efficiency of *ca.* 52% were achieved.²⁸ This electric output is attributed to the breaking of oxygen-hydrogen bonds in carboxyl (COOH) groups, as well as gradient separation of H^+ and COO^- groups on the GO skeleton.^{99,100} The generated potential arising from the downward motion of H^+ and upward motion of oxygen-containing groups causes free electrons to move along the external circuit. In contrast to symmetric structures, a functionalized GO paper with asymmetric electrodes used as a moisture-electric power generator supplied a voltage of 2.0 V.¹⁰¹ Such a high voltage is produced by the asymmetric moisturization of GO, which allows the directional migration of ions across the GO paper. These technologies are assumed to be promising for moisture-electric energy transformation using sea breezes with high humidity.

Oxygen-containing groups play a critical role in the moisture-driven generation of electricity. This principle has been further applied to develop a nanopower generator that consisted of porous carbon films or carbon nanotube yarns with different oxygen-containing groups (Fig. 14a).^{29,102} A constant output voltage of 68 mV was obtained after it was exposed to an environment with a high relative humidity of >95%, but the voltage

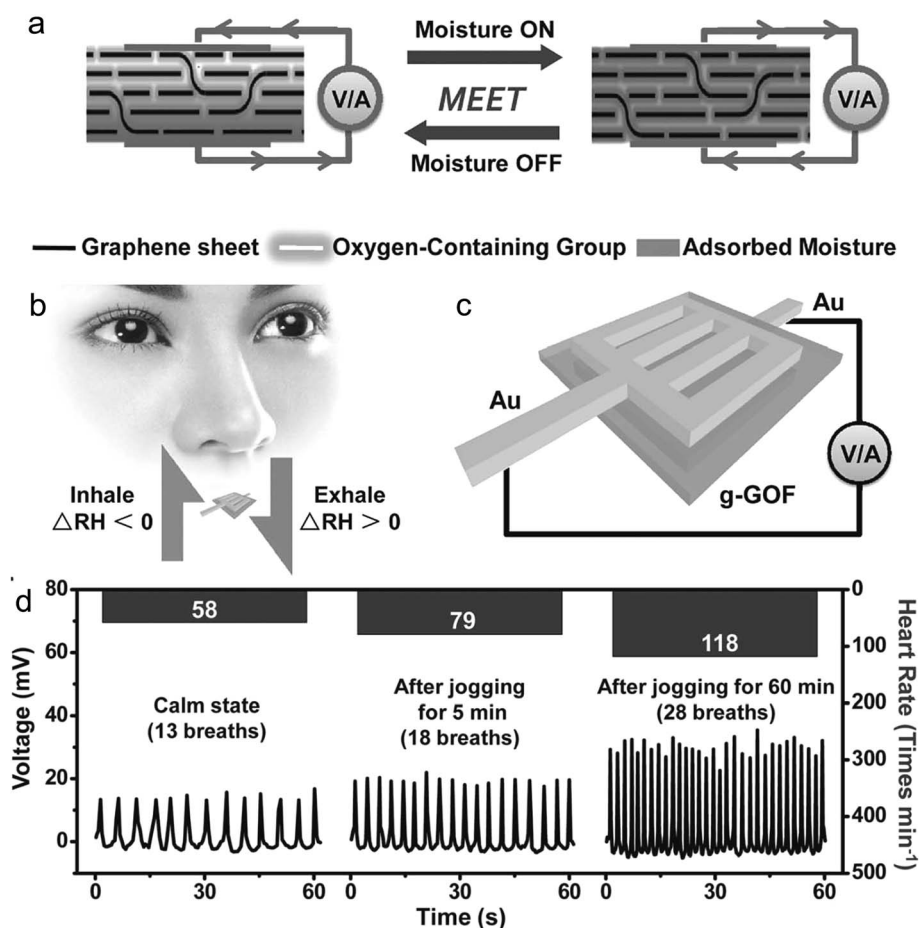


Fig. 13 (a) Self-breathing cycle. (b) Harvesting energy from the body in the flow of respiratory moisture. (c) g-GOF was sandwiched between two gold electrodes. (d) Self-powered monitoring of respiratory frequency related to the heart rate. Reproduced with permission.⁵⁵ Copyright 2015 Wiley-VCH.

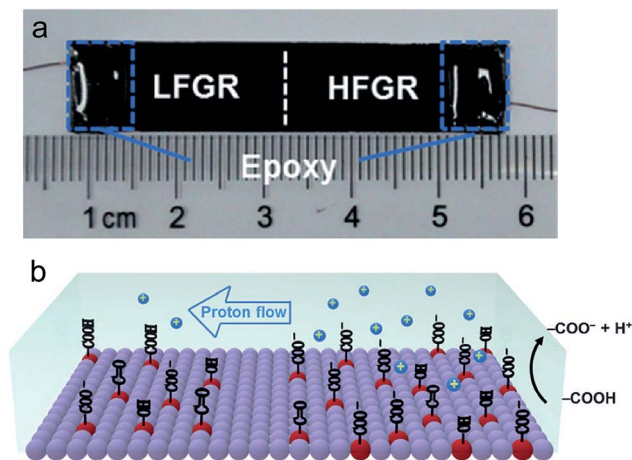


Fig. 14 (a) Photograph of the carbon film device. (b) Proposed mechanism. An imbalance between the release of free protons on the two sides drives the proton flow. Reproduced with permission.²⁹ Copyright 2016 Wiley-VCH.

decreased to zero when the relative humidity decreased to less than 83%. The reproducibility of the performance indicated a strong dependence of the induced voltage on the humidity. However, carbon films in which the two sides had the same content of oxygen-containing groups could not produce electrical potentials. Integrated experiments with simulations revealed that the induced potential originates from the inhomogeneous distribution of functional groups along the film, especially carboxy groups (Fig. 14b). The sufficient number of adsorbed water molecules in porous carbon facilitates the

release of protons from carboxy groups, which results in a drop in potential across the carbon film.

2.3.2. Water evaporation. The evaporation of water is a ubiquitous natural process.^{103–105} The nanoscale confinement of water in hygroscopic materials provides a means of converting evaporation-induced mechanical energy into electricity, which has been utilized in the creation of a number of energy devices.^{56,106–108} Recently, the evaporation of water from the surface of carbon nanomaterials was found to produce electricity.^{27,109,110} The evaporation-induced potential process in a sheet of carbon black is shown in Fig. 15a. TEM images indicate that each of the onion-like nanoparticles is formed of loosely stacked disordered graphene flakes (Fig. 15b and c). In tests, the device was dipped into a beaker with DI water covering the bottom end of the carbon black. The angle of the sheet of carbon black with the water surface was about 57.3°, and the capillary water reached a height of 2.0 cm. Electrical measurements show that evaporation from the centimetre-sized sheet generated a voltage of ~1.0 V under ambient conditions. The induced potential was maintained during the whole test and lasted for 8 days with a stable short-circuit current of around 150 nA in a laboratory environment (Fig. 15d).²⁷ The small fluctuations in the measured voltage were attributed to the fluctuating temperature and humidity.

The interactions between water molecules and carbon layers, and even the evaporation-driven flow of fluids within porous carbon sheets, are thought to be key factors in the generation of potentials. An evaporation-induced potential generates electrical energy from evaporation, which converts sensible energy into latent heat. The generation of electricity is related to traditional streaming potentials, which rely on driving ionic

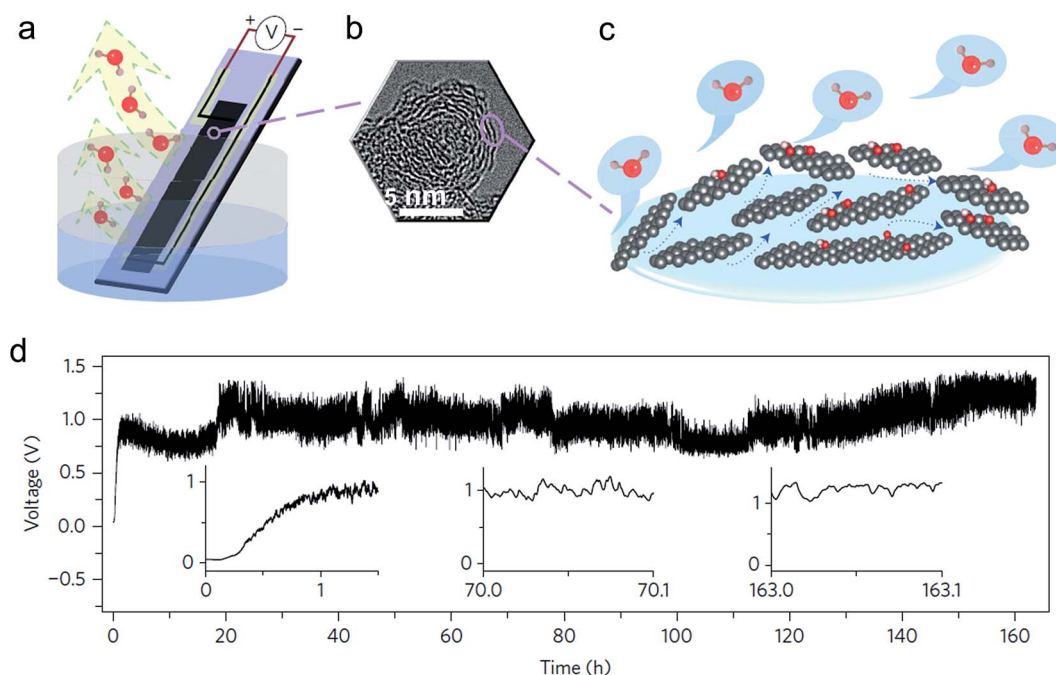


Fig. 15 (a) Evaporation-induced electricity in carbon black film. (b) TEM image of carbon black. (c) Evaporation-induced flow in carbon black. (d) Open-circuit voltage generated by evaporation of water under ambient conditions. Reproduced with permission.²⁷ Copyright 2017 Nature Publishing Group.

Table 1 Summary of blue energy harvesting from water-carbon interfaces

Type	Material(s)	Preparation	Substrate	Solution	Velocity	Potential	Current	Mechanism	Researcher	Ref.
Sliding droplet	Monolayer graphene	CVD	Polyethylene terephthalate	0.6 M NaCl aqueous solution	2.25 cm s ⁻¹	0.15 mV	—	Pseudocapacitance	Yin <i>et al.</i> (2014)	22
Sliding droplet	Monolayer graphene	CVD	SiO ₂ (90 nm)/Si	DI water, 0.5 mg mL ⁻¹ GO aqueous solution	4.0 cm s ⁻¹	0.22 mV	—	Coulomb interaction	Zhong <i>et al.</i> (2015)	64
Sliding droplet	Monolayer graphene	CVD	Polyvinylidene fluoride	DI water	—	0.1 V	—	Piezoelectric charges	Zhong <i>et al.</i> (2017)	36
Sliding droplet	Monolayer graphene	CVD	Polytetrafluoroethylene	0.6 M NaCl solution	—	0.4 V	4.8 μA	Triboelectric effect	Kim <i>et al.</i> (2016)	65
Raining	Reduced graphene oxide	Hummers method	Polyethylene terephthalate	NaCl aqueous solution	20–30 cm s ⁻¹	0.15 mV	0.54 μA	Pseudocapacitance	Tang <i>et al.</i> (2016)	68
Raining	Monolayer graphene, graphene oxide	Electrophoresis	Glass or indium tin oxide/polyethylene terephthalate	0.6 M NaCl	40–100 mL h ⁻¹	62 μV	4.9 μA	Pseudocapacitance	Zhang <i>et al.</i> (2016)	70
Raining	Monolayer graphene	CVD	SiO ₂ /Si	DI water	—	2.54 mV	—	Doping and dedoping	Zhong <i>et al.</i> (2016)	72
Raining	Graphene and carbon black/PTFE sheet	Wet chemistry	Pt or PtNi alloy	0.6 M NaCl	100 mL h ⁻¹	78 μV	0.75 μA	Pseudocapacitance	Tang <i>et al.</i> (2016)	23
Waving	Graphene sheet	CVD	Polyethylene terephthalate	0.6 M NaCl	0–40 cm s ⁻¹	0.1 V	11 μA	Charge transfer by moving the boundary of electric double-layer	Yin <i>et al.</i> (2014)	54
Shaking	Monolayer graphene	CVD	SiO ₂ (90 nm)/Si	DI water, 0.5 mg mL ⁻¹ GO aqueous solution	Slight shaking	10 mV	0.5 μA	Coulomb interaction	Zhong <i>et al.</i> (2015)	64
Circling	MWCNT yarn		Electrochemical cell	0.1 M HCl	—	85 mV	—	Electrochemical conversion of tensile or torsional mechanical energy into electrical energy	Kim <i>et al.</i> (2017)	76
Flowing	SWNT bundles	Electric arc method	Metal electrode	Water, HCl, glycerol	10 ⁻⁵ to 10 ⁻¹ cm s ⁻¹	0.16–9.2 mV	—	Direct forcing of free charge carriers in nanotubes by fluctuating coulombic field	Ghosh <i>et al.</i> (2003)	24
Flowing	Aligned MWCNT fiber		Polymer fiber	0.6 M NaCl	0–200 cm s ⁻¹	0–160 mV	0–22 μA	The charge imbalance removes electrons from the MWCNTs to balance the excess charges	Xu <i>et al.</i> (2017)	83
Flowing	Graphene film	CVD	SiO ₂ /Si	0.6 M HCl	10 cm s ⁻¹	30 mV	—	Net drift velocity of adsorbed ions	Dhiman <i>et al.</i> (2011)	26
Flowing	Graphene sheet	CVD	SiO ₂ /Si or polyethylene terephthalate	0.6 M HCl	1–5 cm s ⁻¹	175 mV	—	Exposure of electrodes	Yin <i>et al.</i> (2012)	84
Flowing	Monolayer graphene	CVD	Glass wafer	DI water	3 cm s ⁻¹	2.68 mV	—	Momentum transferred from the flowing liquid to graphene	Lee <i>et al.</i> (2013)	85
Flowing	Graphene grid	CVD	Flexible polydimethylsiloxane	0.6 M NaCl	4.7–10.6 cm s ⁻¹	118 μV	—	Pseudocapacitor splits the continuous fluid into droplets	He <i>et al.</i> (2015)	87

Table 1 (Contd.)

Type	Material(s)	Preparation	Substrate	Solution	Velocity	Potential	Current	Mechanism	Researcher	Ref.
Flowing	Graphene foam	CVD	Porous nickel	Water	10–60 cm s ⁻¹	—	25 μA	Coupling of molecules in flowing water with charge carriers in graphene at the interface	Huang <i>et al.</i> (2014)	89
Flowing	Graphene foam	CVD	Porous nickel	Ethanol/water mixture	0–60 cm s ⁻¹	—	20 μA	Coupling of molecules in the flowing solution with charge carriers in graphene	Huang <i>et al.</i> (2014)	88
Flowing	Graphene hydrogel membrane	Vacuum filtration	—	0.1 M NaCl	—	—	2.23 nA	Streaming ion current by selective transport of counterions	Guo <i>et al.</i> (2013)	91
Flowing	Graphene oxide	Hummers method	Whatman filter paper	DI water–NaCl, KCl, MgCl ₂	10 cm s ⁻¹	221 mV	325 mA cm ⁻²	Redox mechanism by effective charge separation and faster ion mobility over rGO deposited on a paper surface	Arun <i>et al.</i> (2013)	92
Adsorption	Gradient graphene oxide film	Vacuum filtration	Gold electrode	Moisture	—	20 mV	—	The ionic and electronic conductivities of GO vary with changes in relative humidity	Zhao <i>et al.</i> (2013)	55
Adsorption	GO nanoribbon	Freezing, self-assembly	Al electrode	Moisture	—	50 mV	—	The ionic and electronic conductivities of GO vary with changes in humidity	Zhao <i>et al.</i> (2016)	94
Adsorption	Gradient graphene oxide frameworks	Freeze-drying strategy	Al electrode	Moisture	—	1.3 V	10.5 mA	Diffusion of water molecules to produce dissociated ions as free carriers	Zhao <i>et al.</i> (2016)	28
Adsorption	Porous carbon film	Ethanol flame method	Al ₂ O ₃ ceramic plate	Water vapor	—	60 mV	—	Adsorbed water molecules in porous carbon facilitate the release of protons from carboxy groups	Liu <i>et al.</i> (2016)	29
Evaporation	Carbon black film	Ethanol flame method	Quartz substrate	DI water	—	1.0 V	—	Evaporation-induced potential generates electrical energy from evaporation	Xue <i>et al.</i> (2017)	27
Evaporation	Robust carbon black film	Printing method	Al ₂ O ₃ ceramic plate	DI water	—	1.0 V	3.55 μA	Evaporation-induced potential	Ding <i>et al.</i> (2017)	110

solutions through narrow gaps or moving ionic solutions across graphene surfaces. Besides power generation, it is also possible to design devices for simultaneous solar-powered desalination and electricity generation under natural sunlight. By employing a hybrid system based on a piece of carbon nanotube-modified filter paper and a commercial Nafion membrane, a solar thermal efficiency of 75% and a derived additional electric power of 1 W m^{-2} were achieved under one-sun illumination.¹¹¹ The theoretical power due to the difference in salinity between surface water and bulk seawater could be 12.5 W m^{-2} . As the evaporation of water from graphene materials could be optimized,^{112,113} evaporation-induced potentials could be further increased. Evaporation-driven generators have potential for applications in warm regions of the Earth.

3. Summary and prospects

Electric power is indispensable in our daily life. Water-carbon interfaces with the ability to release the potential energy stored in water are attractive for the development of renewable energy. Such energy conversion relies on either flowing water or specially designed ionic solutions. Here, we summarize experimental advances in, as well as the physical understanding of, the harvesting of energy from water-carbon interfaces and illustrate their key features for power generation. We focus our discussion on three forms of the motion of water that are essential for energy harvesting, namely, the movement of droplets, flow of water and phase changes. Intriguing examples are selected to demonstrate conceptual developments, which include sliding droplets, rain, waves, shaking or flowing water, the adsorption of moisture and evaporation of water. The types of nanogenerators, carbon materials, preparation methods and substrates and their underlying mechanisms, as well as their electricity harvesting properties, are summarized in Table 1. Although research into blue nanopower is in its initial stage, great achievements have been made in producing electric signals using carbon films or porous graphene frameworks. Major experiments show the possibility of converting nanofluidic energy on carbon into electrical energy. A framework has been established to interpret the phenomena of energy harvesting. However, the induced electrical signals are still of the order of mV, which is not suitable for practical applications. Because the size, functional groups and charge properties of the carbon backbones and their derivatives can be intentionally controlled to finely tune the microstructures and chemistries of materials and therefore unlock the potential of tailoring their electrochemical and electrical properties, further optimization of electric output can be expected *via* judicious tailoring of carbon nanomaterials and the systematic design and scaling-up of device structures.

To realize the dream of blue energy, some challenges regarding its empirical and physical aspects still need investigation. Future studies are likely to determine its physical mechanisms in detail to identify key parameters for electricity generation. Besides, novel design concepts, the controlled synthesis of nanomaterials and the assembly of devices are interesting aspects to be investigated. Advanced manufacturing

processes such as wet-chemistry synthesis, low-cost deposition of materials and large-scale self-assembly are required to meet the goals of this technology. The careful design of experimental setups and proper use of molecular simulation techniques would be helpful to reconcile apparent contradictions and provide insights. A unified model that describes the complex interactions between water, carbon materials and substrates and a standard for calibrating the performance of devices are urgently needed. For practical applications of water-carbon systems, a nanogenerator network represents a feasible strategy.^{7,114,115} The connection of units in series would increase the open-circuit voltage, and parallel connection would increase the short-circuit current.^{54,73} Networks that link large numbers of units *via* cables can be mounted on a house roof, float on the surface of water or be located beneath water at a certain depth for harvesting blue energy. Because direct contact with water is required for harvesting blue energy, corrosion problems affect the reliability of devices when the motion of water is used as an energy source. Therefore, the packaging of a device will be vitally important to make it usable in a variety of harsh environments. If the packaging is not robust enough, the movement of water may severely affect performance or even quickly destroy the materials and device. The development of new materials and effective packaging technology and the optimization of modes of operation would be good choices. Moreover, some water contains contamination that may have a negative impact on electricity generation. With respect to environmental considerations, active efforts to seek effective ways to treat contaminated wastewater whilst generating electricity may also upgrade the capability of blue energy systems. As substantial progress has already been made, we anticipate that the dream of blue energy could one day come true and lead to a paradigm shift for practical applications in our daily lives.

Conflicts of interest

The authors declare no competing financial interest.

Acknowledgements

The research was supported by grants from the Natural Science Foundation of China (51576002) and the Norwegian Research Council-Independent Projects-Mathematics, Physical Science and Technology Programme (FRINATEK-231416/F20).

References

- 1 J. Chen, Y. Huang, N. Zhang, H. Zou, R. Liu, C. Tao, X. Fan and Z. L. Wang, Micro-cable structured textile for simultaneously harvesting solar and mechanical energy, *Nat. Energy*, 2016, **1**, 16138.
- 2 Y. Zi, L. Lin, J. Wang, S. Wang, J. Chen, X. Fan, P. K. Yang, F. Yi and Z. L. Wang, Triboelectric-pyroelectric-piezoelectric hybrid cell for high-efficiency energy-harvesting and self-powered sensing, *Adv. Mater.*, 2015, **27**, 2340–2347.

- 3 G. Zhu, J. Chen, T. Zhang, Q. Jing and Z. L. Wang, Radial-arrayed rotary electrification for high performance triboelectric generator, *Nat. Commun.*, 2014, **5**, 3426.
- 4 X. Fan, J. Chen, J. Yang, P. Bai, Z. Li and Z. L. Wang, Ultrathin, rollable, paper-based triboelectric nanogenerator for acoustic energy harvesting and self-powered sound recording, *ACS Nano*, 2015, **9**, 4236–4243.
- 5 J. Chen, G. Zhu, W. Yang, Q. Jing, P. Bai, Y. Yang, T. C. Hou and Z. L. Wang, Harmonic-resonator-based triboelectric nanogenerator as a sustainable power source and a self-powered active vibration sensor, *Adv. Mater.*, 2013, **25**, 6094–6099.
- 6 L. Jin, J. Chen, B. Zhang, W. Deng, L. Zhang, H. Zhang, X. Huang, M. Zhu, W. Yang and Z. L. Wang, Self-Powered Safety Helmet Based on Hybridized Nanogenerator for Emergency, *ACS Nano*, 2016, **10**, 7874–7881.
- 7 J. Chen, J. Yang, Z. Li, X. Fan, Y. Zi, Q. Jing, H. Guo, Z. Wen, K. C. Pradel, S. Niu and Z. L. Wang, Networks of triboelectric nanogenerators for harvesting water wave energy: a potential approach toward blue energy, *ACS Nano*, 2015, **9**, 3324–3331.
- 8 J. A. Paradiso and T. Starner, Energy scavenging for mobile and wireless electronics, *IEEE Pervasive computing*, 2005, **4**, 18–27.
- 9 M. Ye, Z. Zhang, Y. Zhao and L. Qu, Graphene Platforms for Smart Energy Generation and Storage, *Joule*, 2018, **2**, 245–268.
- 10 K. V. Selvan and M. S. Mohamed Ali, Micro-scale energy harvesting devices: Review of methodological performances in the last decade, *Renewable Sustainable Energy Rev.*, 2016, **54**, 1035–1047.
- 11 J. J. Urban, Emerging Scientific and Engineering Opportunities within the Water-Energy Nexus, *Joule*, 2017, **1**, 665–688.
- 12 F. R. Fan, W. Tang and Z. L. Wang, Flexible Nanogenerators for Energy Harvesting and Self-Powered Electronics, *Adv. Mater.*, 2016, **28**, 4283–4305.
- 13 A. S. Bahaj, Generating electricity from the oceans, *Renewable Sustainable Energy Rev.*, 2011, **15**, 3399–3416.
- 14 Z. L. Wang, New wave power, *Nature*, 2017, **542**, 159–160.
- 15 A. Striolo, A. Michaelides and L. Joly, The Carbon-Water Interface: Modeling Challenges and Opportunities for the Water-Energy Nexus, *Annu. Rev. Chem. Biomol. Eng.*, 2016, **7**, 533–556.
- 16 H. G. Park and Y. Jung, Carbon nanofluidics of rapid water transport for energy applications, *Chem. Soc. Rev.*, 2014, **43**, 565–576.
- 17 C. Hu, L. Song, Z. Zhang, N. Chen, Z. Feng and L. Qu, Tailored graphene systems for unconventional applications in energy conversion and storage devices, *Energy Environ. Sci.*, 2015, **8**, 31–54.
- 18 M. S. Joseph Prudell, E. Amon, T. K. A. Brekken and A. von Jouanne, A Permanent-Magnet Tubular Linear Generator for Ocean Wave Energy Conversion, *IEEE Trans. Ind. Appl.*, 2010, **46**, 2392–2400.
- 19 X. Chen, B. Xu and L. Liu, Nanoscale Fluid Mechanics and Energy Conversion, *Appl. Mech. Rev.*, 2014, **66**, 050803.
- 20 Z. L. Wang, On Maxwell's displacement current for energy and sensors: the origin of nanogenerators, *Mater. Today*, 2017, **20**, 74–82.
- 21 Y. Z. Weiping Li and C. Pan, Graphene-based Nanogenerator Experiments, Theories and Applications, *Mater. Res. Soc. Symp. Proc.*, 2015, **1782**, 15–21.
- 22 J. Yin, X. Li, J. Yu, Z. Zhang, J. Zhou and W. Guo, Generating electricity by moving a droplet of ionic liquid along graphene, *Nat. Nanotechnol.*, 2014, **9**, 378–383.
- 23 Q. W. Tang, H. N. Zhang, B. L. He and P. Z. Yang, An all-weather solar cell that can harvest energy from sunlight and rain, *Nano Energy*, 2016, **30**, 818–824.
- 24 S. Ghosh, A. K. Sood and N. Kumar, Carbon nanotube flow sensors, *Science*, 2003, **299**, 1042–1044.
- 25 Q. Yuan and Y. P. Zhao, Hydroelectric voltage generation based on water-filled single-walled carbon nanotubes, *J. Am. Chem. Soc.*, 2009, **131**, 6374–6376.
- 26 P. Dhiman, F. Yavari, X. Mi, H. Gullapalli, Y. Shi, P. M. Ajayan and N. Koratkar, Harvesting energy from water flow over graphene, *Nano Lett.*, 2011, **11**, 3123–3127.
- 27 G. Xue, Y. Xu, T. Ding, J. Li, J. Yin, W. Fei, Y. Cao, J. Yu, L. Yuan, L. Gong, J. Chen, S. Deng, J. Zhou and W. Guo, Water-evaporation-induced electricity with nanostructured carbon materials, *Nat. Nanotechnol.*, 2017, **12**, 317–321.
- 28 F. Zhao, Y. Liang, H. H. Cheng, L. Jiang and L. T. Qu, Highly efficient moisture-enabled electricity generation from graphene oxide frameworks, *Energy Environ. Sci.*, 2016, **9**, 912–916.
- 29 K. Liu, P. Yang, S. Li, J. Li, T. Ding, G. Xue, Q. Chen, G. Feng and J. Zhou, Induced Potential in Porous Carbon Films through Water Vapor Absorption, *Angew. Chem.*, 2016, **55**, 8003–8007.
- 30 Y. Zhai, Y. Dou, D. Zhao, P. F. Fulvio, R. T. Mayes and S. Dai, Carbon materials for chemical capacitive energy storage, *Adv. Mater.*, 2011, **23**, 4828–4850.
- 31 S. L. Candelaria, Y. Shao, W. Zhou, X. Li, J. Xiao, J.-G. Zhang, Y. Wang, J. Liu, J. Li and G. Cao, Nanostructured carbon for energy storage and conversion, *Nano Energy*, 2012, **1**, 195–220.
- 32 H. Jiang, P. S. Lee and C. Li, 3D carbon based nanostructures for advanced supercapacitors, *Energy Environ. Sci.*, 2013, **6**, 41–53.
- 33 Q. Ma, Y. Yu, M. Sindoro, A. G. Fane, R. Wang and H. Zhang, Carbon-Based Functional Materials Derived from Waste for Water Remediation and Energy Storage, *Adv. Mater.*, 2017, **29**, 1605361.
- 34 Z. Liu, Advances in electrokinetics revealed in graphene, *Natl. Sci. Rev.*, 2015, **2**, 17–18.
- 35 L. D'Urso, C. Satriano, G. Forte, G. Compagnini and O. Puglisi, Water structure and charge transfer phenomena at the liquid-graphene interface, *Phys. Chem. Chem. Phys.*, 2012, **14**, 14605–14610.
- 36 H. K. Zhong, J. Xia, F. C. Wang, H. S. Chen, H. Z. G. Wu and S. S. Lin, Graphene-Piezoelectric Material Heterostructure for Harvesting Energy from Water Flow, *Adv. Funct. Mater.*, 2017, **27**, 1604226.

- 37 Y. Xu, P. Chen and H. Peng, Generating Electricity from Water through Carbon Nanomaterials, *Chem.–Eur. J.*, 2018, **24**, 6287–6294.
- 38 Q. Xie, M. A. Alibakhshi, S. Jiao, Z. Xu, M. Hempel, J. Kong, H. G. Park and C. Duan, Fast water transport in graphene nanofluidic channels, *Nat. Nanotechnol.*, 2018, **13**, 238–245.
- 39 G. Liu, W. Jin and N. Xu, Graphene-based membranes, *Chem. Soc. Rev.*, 2015, **44**, 5016–5030.
- 40 N. Wei, X. Peng and Z. Xu, Understanding water permeation in graphene oxide membranes, *ACS Appl. Mater. Interfaces*, 2014, **6**, 5877–5883.
- 41 A. R. Koltonow and J. Huang, Ionic Transport, Two-dimensional nanofluidics, *Science*, 2016, **351**, 1395–1396.
- 42 E. Secchi, S. Marbach, A. Nigues, D. Stein, A. Siria and L. Bocquet, Massive radius-dependent flow slippage in carbon nanotubes, *Nature*, 2016, **537**, 210–213.
- 43 C. Cheng, G. Jiang, C. J. Garvey, Y. Wang, G. P. Simon, J. Z. Liu and D. Li, Ion transport in complex layered graphene-based membranes with tuneable interlayer spacing, *Sci. Adv.*, 2016, **2**, e1501272.
- 44 R. B. Schoch, J. Han and P. Renaud, Transport phenomena in nanofluidics, *Rev. Mod. Phys.*, 2008, **80**, 839–883.
- 45 C. Y. Lee, W. Choi, J. H. Han and M. S. Strano, Coherence resonance in a single-walled carbon nanotube ion channel, *Science*, 2010, **329**, 1320–1324.
- 46 L. Bocquet and R. R. Netz, Nanofluidics: Phonon modes for faster flow, *Nat. Nanotechnol.*, 2015, **10**, 657–658.
- 47 M. Whitby and N. Quirke, Fluid flow in carbon nanotubes and nanopipes, *Nat. Nanotechnol.*, 2007, **2**, 87–94.
- 48 P. Kral and M. Shapiro, Nanotube Electron Drag in Flowing Liquids, *Phys. Rev. Lett.*, 2001, **86**, 131–134.
- 49 J. Kim, J. Lee, S. Kim and W. Jung, Highly Increased Flow-Induced Power Generation on Plasmonically Carbonized Single-Walled Carbon Nanotube, *ACS Appl. Mater. Interfaces*, 2016, **8**, 29877–29882.
- 50 B. N. J. Persson, U. Tartaglino, E. Tosatti and H. Ueba, Electronic friction and liquid-flow-induced voltage in nanotubes, *Phys. Rev. B: Condens. Matter Mater. Phys.*, 2004, **69**, 1681–1685.
- 51 Q. Shao, J. Jia, Y. Guan, X. He and X. Zhang, Flow-induced voltage generation by moving a nano-sized ionic liquids droplet over a graphene sheet: Molecular dynamics simulation, *J. Chem. Phys.*, 2016, **144**, 124703.
- 52 W. Sparreboom, A. van den Berg and J. C. Eijkel, Principles and applications of nanofluidic transport, *Nat. Nanotechnol.*, 2009, **4**, 713–720.
- 53 D. Nandi, A. D. Finck, J. P. Eisenstein, L. N. Pfeiffer and K. W. West, Exciton condensation and perfect Coulomb drag, *Nature*, 2012, **488**, 481–484.
- 54 J. Yin, Z. Zhang, X. Li, J. Yu, J. Zhou, Y. Chen and W. Guo, Waving potential in graphene, *Nat. Commun.*, 2014, **5**, 3582.
- 55 F. Zhao, H. Cheng, Z. Zhang, L. Jiang and L. Qu, Direct Power Generation from a Graphene Oxide Film under Moisture, *Adv. Mater.*, 2015, **27**, 4351–4357.
- 56 X. Chen, D. Goodnight, Z. Gao, A. H. Cavusoglu, N. Sabharwal, M. DeLay, A. Driks and O. Sahin, Scaling up nanoscale water-driven energy conversion into evaporation-driven engines and generators, *Nat. Commun.*, 2015, **6**, 7346.
- 57 K. Liu, T. Ding, J. Li, Q. Chen, G. Xue, P. Yang, M. Xu, Z. L. Wang and J. Zhou, Thermal-Electric Nanogenerator Based on the Electrokinetic Effect in Porous Carbon Film, *Adv. Energy Mater.*, 2018, 1702481.
- 58 Q. W. Tang and P. Z. Yang, The era of water-enabled electricity generation from graphene, *J. Mater. Chem. A*, 2016, **4**, 9730–9738.
- 59 B. E. Logan and M. Elimelech, Membrane-based processes for sustainable power generation using water, *Nature*, 2012, **488**, 313–319.
- 60 M. Elimelech and W. A. Phillip, The future of seawater desalination: energy, technology, and the environment, *Science*, 2011, **333**, 712–717.
- 61 Y. S. Shanshan Yang, Y. Xu, Q. Wu, Y. Zhang, M. B. Raschke, M. Ren, Y. Chen, J. Wang, W. Guo, Y. Ron Shen and C. Tian, Mechanism of Electric Power Generation from Ionic Droplet Motion on Polymer Supported Graphene, arXiv:1801.07878, 2018.
- 62 T. Brousse, D. Belanger and J. W. Long, To Be or Not To Be Pseudocapacitive?, *J. Electrochem. Soc.*, 2015, **162**, A5185–A5189.
- 63 A. K. Geim and I. V. Grigorieva, van der Waals heterostructures, *Nature*, 2013, **499**, 419–425.
- 64 H. Zhong, X. Li, Z. Wu, S. Zhang, Z. Xu, H. Chen and S. Lin, Two dimensional graphene nanogenerator by coulomb dragging: Moving van der Waals heterostructure, *Appl. Phys. Lett.*, 2015, **106**, 243903.
- 65 S. S. Kwak, S. Lin, J. H. Lee, H. Ryu, T. Y. Kim, H. Zhong, H. Chen and S. W. Kim, Triboelectrification-Induced Large Electric Power Generation from a Single Moving Droplet on Graphene/Polytetrafluoroethylene, *ACS Nano*, 2016, **10**, 7297–7302.
- 66 Q. J. Liang, X. Q. Yan, X. Q. Liao and Y. Zhang, Integrated multi-unit transparent triboelectric nanogenerator harvesting rain power for driving electronics, *Nano Energy*, 2016, **25**, 18–25.
- 67 Q. Tang, Y. Duan, B. He and H. Chen, Platinum Alloy Tailored All-Weather Solar Cells for Energy Harvesting from Sun and Rain, *Angew. Chem.*, 2016, **55**, 14412–14416.
- 68 Q. Tang, X. Wang, P. Yang and B. He, A Solar Cell That Is Triggered by Sun and Rain, *Angew. Chem.*, 2016, **128**, 5329–5332.
- 69 J. Duan, T. Hu, Y. Zhao, B. He and Q. Tang, Carbon-Electrode-Tailored All-Inorganic Perovskite Solar Cells To Harvest Solar and Water-Vapor Energy, *Angew. Chem.*, 2018, **130**, 5848–5851.
- 70 Y. Zhang, Q. W. Tang, B. L. He and P. Z. Yang, Graphene enabled all-weather solar cells for electricity harvest from sun and rain, *J. Mater. Chem. A*, 2016, **4**, 13235–13241.
- 71 J. Li, K. Liu, G. Xue, T. Ding, P. Yang, Q. Chen, Y. Shen, S. Li, G. Feng, A. Shen, M. Xu and J. Zhou, Electricity generation from water droplets via capillary infiltrating, *Nano Energy*, 2018, **48**, 211–216.
- 72 H. Zhong, Z. Wu, X. Li, W. Xu, S. Xu, S. Zhang, Z. Xu, H. Chen and S. Lin, Graphene based two dimensional

- hybrid nanogenerator for concurrently harvesting energy from sunlight and water flow, *Carbon*, 2016, **105**, 199–204.
- 73 X. M. Li, C. Shen, Q. Wang, C. M. Luk, B. W. Li, J. Yin, S. P. Lau and W. L. Guo, Hydroelectric generator from transparent flexible zinc oxide nanofilms, *Nano Energy*, 2017, **32**, 125–129.
- 74 J. Tan, J. Duan, Y. Zhao, B. He and Q. Tang, Generators to harvest ocean wave energy through electrokinetic principle, *Nano Energy*, 2018, **48**, 128–133.
- 75 S. H. Kim, M. D. Lima, M. E. Kozlov, C. S. Haines, G. M. Spinks, S. Aziz, C. Choi, H. J. Sim, X. Wang, H. Lu, D. Qian, J. D. W. Madden, R. H. Baughman and S. J. Kim, Harvesting temperature fluctuations as electrical energy using torsional and tensile polymer muscles, *Energy Environ. Sci.*, 2015, **8**, 3336–3344.
- 76 S. H. Kim, C. S. Haines, N. Li, K. J. Kim, T. J. Mun, C. Choi, J. Di, Y. J. Oh, J. P. Oviedo, J. Bykova, S. Fang, N. Jiang, Z. Liu, R. Wang, P. Kumar, R. Qiao, S. Priya, K. Cho, M. Kim, M. S. Lucas, L. F. Drummy, B. Maruyama, D. Y. Lee, X. Lepro, E. Gao, D. Albarq, R. Ovalle-Robles, S. J. Kim and R. H. Baughman, Harvesting electrical energy from carbon nanotube yarn twist, *Science*, 2017, **357**, 773–778.
- 77 S. Ghosh, A. Sood, S. Ramaswamy and N. Kumar, Flow-induced voltage and current generation in carbon nanotubes, *Phys. Rev. B: Condens. Matter Mater. Phys.*, 2004, **70**, 3352–3359.
- 78 S. H. Lee, D. Kim, S. Kim and C. S. Han, Flow-induced voltage generation in high-purity metallic and semiconducting carbon nanotubes, *Appl. Phys. Lett.*, 2011, **99**, 104103.
- 79 A. E. Cohen, Carbon nanotubes provide a charge, *Science*, 2003, **300**, 1235–1236.
- 80 J. Park, S. Song, C. Shin, Y. Yang, S. A. L. Weber, E. Sim and Y. S. Kim, Ion Specificity on Electric Energy Generated by Flowing Water Droplets, *Angew. Chem.*, 2018, **57**, 2091–2095.
- 81 Y. Zhao, L. Song, K. Deng, Z. Liu, Z. Zhang, Y. Yang, C. Wang, H. Yang, A. Jin, Q. Luo, C. Gu, S. Xie and L. Sun, Individual Water-Filled Single-Walled Carbon Nanotubes as Hydroelectric Power Converters, *Adv. Mater.*, 2008, **20**, 1772–1776.
- 82 A. K. Sood and S. Ghosh, Direct Generation of a Voltage and Current by Gas Flow Over Carbon Nanotubes and Semiconductors, *Phys. Rev. Lett.*, 2004, **93**, 086601.
- 83 Y. Xu, P. Chen, J. Zhang, S. Xie, F. Wan, J. Deng, X. Cheng, Y. Hu, M. Liao, B. Wang, X. Sun and H. Peng, A One-Dimensional Fluidic Nanogenerator with a High Power Conversion Efficiency, *Angew. Chem.*, 2017, **56**, 12940–12945.
- 84 J. Yin, Z. Zhang, X. Li, J. Zhou and W. Guo, Harvesting Energy from Water Flow over Graphene?, *Nano Lett.*, 2012, **12**, 1736–1741.
- 85 S. H. Lee, Y. Jung, S. Kim and C. S. Han, Flow-induced voltage generation in non-ionic liquids over monolayer graphene, *Appl. Phys. Lett.*, 2013, **102**, 063116.
- 86 S. H. Lee, Y. B. Kang, W. Jung, Y. Jung, S. Kim and H. M. Noh, Flow-induced voltage generation over monolayer graphene in the presence of herringbone grooves, *Nanoscale Res. Lett.*, 2013, **8**, 487.
- 87 Y. J. He, J. C. Lao, T. T. Yang, X. Li, X. B. Zang, X. M. Li, M. Zhu, Q. Chen, M. L. Zhong and H. W. Zhu, Galvanism of continuous ionic liquid flow over graphene grids, *Appl. Phys. Lett.*, 2015, **107**, 081605.
- 88 W. B. Huang, G. L. Wang, F. Q. Gao, Z. T. Qiao, G. Wang, M. J. Chen, Y. Deng, L. Tao, Y. Zhao, X. K. Fan and L. F. Sun, Energy Harvesting from the Mixture of Water and Ethanol Flowing through Three-Dimensional Graphene Foam, *J. Phys. Chem. C*, 2014, **118**, 8783–8787.
- 89 W. Huang, G. Wang, F. Gao, Z. Qiao, G. Wang, L. Tao, M. Chen, F. Yu, H. Yang and L. Sun, Power generation from water flowing through three-dimensional graphene foam, *Nanoscale*, 2014, **6**, 3921–3924.
- 90 L. Huang, J. Pei, H. Jiang, C. Li and X. Hu, Electricity generation across graphene oxide membranes, *Mater. Res. Bull.*, 2018, **97**, 96–100.
- 91 W. Guo, C. Cheng, Y. Wu, Y. Jiang, J. Gao, D. Li and L. Jiang, Bio-inspired two-dimensional nanofluidic generators based on a layered graphene hydrogel membrane, *Adv. Mater.*, 2013, **25**, 6064–6068.
- 92 R. K. Arun, P. Singh, G. Biswas, N. Chanda and S. Chakraborty, Energy generation from water flow over a reduced graphene oxide surface in a paper-pencil device, *Lab Chip*, 2016, **16**, 3589–3596.
- 93 J. L. Xue, F. Zhao, C. G. Hu, Y. Zhao, H. X. Luo, L. M. Dai and L. T. Qu, Vapor-Activated Power Generation on Conductive Polymer, *Adv. Funct. Mater.*, 2016, **26**, 8784–8792.
- 94 F. Zhao, L. Wang, Y. Zhao, L. Qu and L. Dai, Graphene Oxide Nanoribbon Assembly toward Moisture-Powered Information Storage, *Adv. Mater.*, 2017, **29**, 1604972.
- 95 H. Cheng, Y. Huang, F. Zhao, C. Yang, P. Zhang, L. Jiang, G. Shi and L. Qu, Spontaneous power source in ambient air of a well-directionally reduced graphene oxide bulk, *Energy Environ. Sci.*, 2018, DOI: 10.1039/C8EE01502C.
- 96 H. Cheng, Y. Hu, F. Zhao, Z. Dong, Y. Wang, N. Chen, Z. Zhang and L. Qu, Moisture-activated torsional graphene-fiber motor, *Adv. Mater.*, 2014, **26**, 2909–2913.
- 97 H. Cheng, J. Liu, Y. Zhao, C. Hu, Z. Zhang, N. Chen, L. Jiang and L. Qu, Graphene fibers with predetermined deformation as moisture-triggered actuators and robots, *Angew. Chem.*, 2013, **52**, 10482–10486.
- 98 S. Kim, S. Zhou, Y. Hu, M. Acik, Y. J. Chabal, C. Berger, W. de Heer, A. Bongiorno and E. Riedo, Room-temperature metastability of multilayer graphene oxide films, *Nat. Mater.*, 2012, **11**, 544–549.
- 99 W. Gao, N. Singh, L. Song, Z. Liu, A. L. M. Reddy, L. Ci, R. Vajtai, Q. Zhang, B. Wei and P. M. Ajayan, Direct laser writing of micro-supercapacitors on hydrated graphite oxide films, *Nat. Nanotechnol.*, 2011, **6**, 496–500.
- 100 J. Zhu, H. Zhang and N. A. Kotov, Thermodynamic and structural insights into nanocomposites engineering by comparing two materials assembly techniques for graphene, *ACS Nano*, 2013, **7**, 4818–4829.

- 101 Y. Liang, F. Zhao, Z. Cheng, Y. Deng, Y. Xiao, H. Cheng, P. Zhang, Y. Huang, H. Shao and L. Qu, Electric power generation *via* asymmetric moisturizing of graphene oxide for flexible, printable and portable electronics, *Energy Environ. Sci.*, 2018, **11**, 1703–1735.
- 102 S. He, Y. Zhang, L. Qiu, L. Zhang, Y. Xie, J. Pan, P. Chen, B. Wang, X. Xu, Y. Hu, C. T. Dinh, P. De Luna, M. N. Banis, Z. Wang, T. K. Sham, X. Gong, B. Zhang, H. Peng and E. H. Sargent, Chemical-to-Electricity Carbon: Water Device, *Adv. Mater.*, 2018, **30**, e1707635.
- 103 H. L. Penman, Natural Evaporation from Open Water, Bare Soil and Grass, *Proc. R. Soc. A*, 1948, **193**, 120–145.
- 104 F. Duan, V. K. Badam, F. Durst and C. A. Ward, Thermocapillary transport of energy during water evaporation, *Phys. Rev. E: Stat., Nonlinear, Soft Matter Phys.*, 2005, **72**, 056303.
- 105 A. H. Cavusoglu, X. Chen, P. Gentine and O. Sahin, Potential for natural evaporation as a reliable renewable energy resource, *Nat. Commun.*, 2017, **8**, 617.
- 106 M. Ma, L. Guo, D. G. Anderson and R. Langer, Bio-inspired polymer composite actuator and generator driven by water gradients, *Science*, 2013, **339**, 186–189.
- 107 X. Chen, L. Mahadevan, A. Driks and O. Sahin, Bacillus spores as building blocks for stimuli-responsive materials and nanogenerators, *Nat. Nanotechnol.*, 2014, **9**, 137–141.
- 108 T. D. Wheeler and A. D. Stroock, The transpiration of water at negative pressures in a synthetic tree, *Nature*, 2008, **455**, 208–212.
- 109 Z. Liu, K. Zheng, L. Hu, J. Liu, C. Qiu, H. Zhou, H. Huang, H. Yang, M. Li, C. Gu, S. Xie, L. Qiao and L. Sun, Surface-Energy Generator of Single-Walled Carbon Nanotubes and Usage in a Self-Powered System, *Adv. Mater.*, 2010, **22**, 999–1003.
- 110 T. Ding, K. Liu, J. Li, G. Xue, Q. Chen, L. Huang, B. Hu and J. Zhou, All-Printed Porous Carbon Film for Electricity Generation from Evaporation-Driven Water Flow, *Adv. Funct. Mater.*, 2017, 1700551.
- 111 P. Yang, K. Liu, Q. Chen, J. Li, J. Duan, G. Xue, Z. Xu, W. Xie and J. Zhou, Solar-driven simultaneous steam production and electricity generation from salinity, *Energy Environ. Sci.*, 2017, **10**, 1923–1927.
- 112 Y. Ito, Y. Tanabe, J. Han, T. Fujita, K. Tanigaki and M. Chen, Multifunctional Porous Graphene for High-Efficiency Steam Generation by Heat Localization, *Adv. Mater.*, 2015, **27**, 4302–4307.
- 113 G. P. Hongru Ding, D. Ma, S. W. Sharshir and N. Yang, Ratchet Effect on Gas Transport by Nanoporous Graphene-Significant Enhancement of Vapor Generation, *Mesoscale and Nanoscale Physics*, Cornell University Library, 2017, arXiv:1703.05473v05471.
- 114 Z. L. Wang, T. Jiang and L. Xu, Toward the blue energy dream by triboelectric nanogenerator networks, *Nano Energy*, 2017, **39**, 9–23.
- 115 X. Li, J. Tao, X. Wang, J. Zhu, C. Pan and Z. L. Wang, Networks of High Performance Triboelectric Nanogenerators Based on Liquid-Solid Interface Contact Electrification for Harvesting Low-Frequency Blue Energy, *Adv. Energy Mater.*, 2018, 1800705.